

2011

Vibration Based Technique For Monitoring The Postbuckling Deformation

Bashir Mustafa Ali
North Carolina Agricultural and Technical State University

Follow this and additional works at: <https://digital.library.ncat.edu/dissertations>

Recommended Citation

Ali, Bashir Mustafa, "Vibration Based Technique For Monitoring The Postbuckling Deformation" (2011).
Dissertations. 8.
<https://digital.library.ncat.edu/dissertations/8>

This Dissertation is brought to you for free and open access by the Electronic Theses and Dissertations at Aggie Digital Collections and Scholarship. It has been accepted for inclusion in Dissertations by an authorized administrator of Aggie Digital Collections and Scholarship. For more information, please contact iyanna@ncat.edu.

VIBRATION BASED TECHNIQUE FOR MONITORING
THE POSTBUCKLING DEFORMATION

by

Bashir Mustafa Ali

A dissertation submitted to the graduate faculty
in partial fulfillment of the requirements for the degree of
DOCTOR OF PHILOSOPHY

Department: Mechanical Engineering
Major: Mechanical Engineering
Major Professor: Dr. Mannur J. Sundaresan

North Carolina A&T State University
Greensboro, North Carolina
2011

ABSTRACT

Ali, Bashir M. VIBRATION BASED TECHNIQUE FOR MONITORING THE POSTBUCKLING DEFORMATION. (Major Advisor: Dr. Mannur J Sundaresan), North Carolina Agricultural & Technical State University.

Structural health monitoring (SHM) is a technology whose objective is to detect damage growth in metallic and composite structural elements long before they reach critical dimensions. Most structural health monitoring approaches that have been developed in the past have confined their attention to material degradation such as cracks in metals and delaminations in composite materials. Buckling instability is another cause of catastrophic failure commonly seen in engineering structures. The objective of this study is to develop a technique capable of detecting the onset of buckling instability in structural members and assessing the margin of safety from final collapse. The technique used is based on monitoring vibration characteristics of plate-like structures as they undergo different levels of buckling deformation. A square aluminum panel loaded under uniform shear stresses at the edges is considered for demonstrating the feasibility of this structural health monitoring technique. The buckling loads and the progressively increasing deformation in the post-buckled regime are first determined using finite element analysis. The results from finite element analysis indicate that the natural frequencies as well as mode shapes are highly sensitive to the level of deformation in the post-buckled condition.

The vibration characteristics of the square panel under edge shear loading is also investigated through experiments. The plate is clamped in a “picture-frame” fixture loaded under diagonal compression to simulate edge shear loads, in an Materials Test Systems

(MTS) machine. The transverse deformation pattern is measured at different load levels. The vibration characteristics are measured using a laser vibrometer. The experimental results in general agree with the results from numerical analysis, but there are differences in the mode shapes and frequencies between the experiments and finite element analysis. The differences may be attributable to initial imperfections in the plate, and the inability to apply completely clamped conditions in the experiments. However, the results demonstrate that vibration characteristics can serve as a sensitive indicator for predicting the incipient damage and final collapse of the structural element.

School of Graduate Studies
North Carolina Agricultural and Technical State University

This is to certify that the Doctoral Dissertation of

Bashir Mustafa Ali

has met the dissertation requirements of
North Carolina Agricultural and Technical State University

Greensboro, North Carolina
2011

Approved by:

Dr. Mannur J. Sundaesan
Major Professor

Dr. Albert Esterline
Committee Member

Dr. Devdas Pai
Committee Member

Dr. John Kizito
Committee Member

Dr. Samuel P. Owusu-Ofori
Department Chairperson

Dr. Sanjiv Sarin
Dean of Graduate Studies

DEDICATION

This dissertation is dedicated to my father's soul.

BIOGRAPHICAL SKETCH

Bashir Mustafa Ali was born on January 1, 1958 in Khartoum, Sudan. He attended Khartoum High School. After completing his high school education 1978, he entered the college of engineering at the University of Khartoum, Sudan, where he earned his Bachelor of Science degree in Mechanical Engineering. He was later admitted to the graduate program in Mechanical Engineering at North Carolina Agricultural and Technical State University, Greensboro, North Carolina. He has preformed research on monitoring local instability of composite structures using vibration-based methods. He received his Master of Science degree in Mechanical Engineering in summer of 2004. In the fall of 2006, he was admitted to the Ph.D. program in the department of Mechanical Engineering at North Carolina Agricultural and Technical State University. He continued his research in full research in the field of structural health monitoring. He is currently a candidate for the Doctoral of Philosophy degree in Mechanical Engineering. He has a number of publications in his area of research.

ACKNOWLEDGMENTS

The author wishes to express his deepest appreciation and sincere admiration to his advisor Dr. Mannur J. Sundaresan, for his advice, suggestions, kind support, continued guidance through educational and personally challenging times during my studies at North Carolina Agricultural and Technical State University. In addition, his good intention and limitless patience during research and writing of this dissertation, have been truly invaluable. I wish to express my appreciation to my dissertation committee members, Dr. Devdas M. Pai, Dr. Albert C. Esterline and Dr. John Kizito for their time and critical review of my thesis. Special thanks are also extended to Mr. L. Sripragash, Mr. Kassahun Asamene, Dr. Wesley B. Williams, and Mr. Gene Warwick for sharing their knowledge and for their strong support. I am thankful to Mr. Travis Whitlow and Mr. Travis Knighton for their cooperation. I am grateful for the funding support granted by Army Research Office Grant 50616-EG-H and NASA Grant for the successful completion of this work. Finally, I thank my parents, my wife, my sons, my sister and my brothers for their support, encouragement and love.

TABLE OF CONTENTS

LIST OF FIGURES	ix
LIST OF TABLES.....	xi
LIST OF SYMBOLS.....	xii
CHAPTER 1. INTRODUCTION	1
1.1. Structural Health Monitoring	1
1.2. Buckling Instability in Structural Elements.....	3
1.3. Regions of Postbuckling Deformation.....	4
1.4. Objectives and Scope of the Dissertation	6
1.5. Organization of the Dissertation	7
CHAPTER 2. LITERATURE REVIEW	8
2.1. Introduction.....	8
2.2. Analysis of Buckling Instability	8
2.3. Vibration of Plates and Shells	13
2.4. Vibration of Postbuckled Bars, Beams, and Plates	13
2.5. Structural Health Monitoring Techniques for Detecting the Onset of Buckling.....	15

CHAPTER 3. NUMERICAL ANALYSIS OF POSTBUCKLED DEFORMATION.....	18
3.1. Introduction.....	18
3.2. Classical Approach.....	19
3.3. Numerical Modeling.....	21
3.4. Results of Numerical Analysis.....	23
3.4.1. Validation of the Numerical Results	23
3.4.2. Results for the Aluminum Panel.....	25
3.5. Summary.....	27
CHAPTER 4. NUMERICAL ANALYSIS OF THE VIBRATION CHARACTERISTICS OF THE SHEAR PANEL.....	28
4.1. Introduction.....	28
4.2. Numerical Modeling.....	29
4.3. Results of the Dynamic Analysis.....	30
4.4. Summary.....	36
CHAPTER 5. EXPERIMENTAL DETERMINATION OF VIBRATION CHARACTERISTICS OF POSTBUCKLED SHEAR PANEL	38
5.1. Introduction.....	38
5.2. Experimental Setup	38
5.3. Results.....	43
5.3.1. Static Deflection in the Post Buckled Region.....	43

5.3.2. Dynamic Characteristics in the Postbuckled Region	45
5.4. Summary	56
CHAPTER 6. CONCLUSIONS	58
REFERENCES	60

LIST OF FIGURES

FIGURE	PAGE
1.1. Schematic illustration of deformation and stability in post buckled region of structures.....	5
3.1. Schematic of shear load application. (a) Edge shear. (b) Equivalent corner.....	22
3.2. Comparison of the numerical techniques	24
3.3. Nonlinear buckled plate contour.....	26
3.4. Numerical results of variation of transverse deflection with load	27
4.1. Mode shapes and frequencies of the prebuckled shear panel	31
4.2. Natural frequencies and mode shapes of panel for the load of 1000 lbf	32
4.3. Natural frequencies and mode shapes of panel for the load of 2000 lbf	33
4.4. Comparison of the first five frequencies and mode shapes of panel at different stages of buckling.....	34
4.5. Variation of natural frequencies as a function of applied load	35
5.1. (a) Picture Frame Setup for Shear Loading (b) Effective edge shear (c) Location of the PZT patches for exciting vibration.....	39
5.2. Experimental set-up.....	40
5.3. The transverse deflections of the postbuckled shear panel at different load levels (a) 500 lbf, (b) 1000 lbf, (c) 1500 lbf, and (d) 2000 lbf	43
5.4. Variation of central deflection as a function of applied load.....	44
5.5. Mode shape and frequency comparison for free load conditions	46
5.6. Vibration amplitude spectrum under no load condition.....	47
5.7. Vibration amplitude spectrum for a load of 500 lbf.....	48

5.8.	Mode shape and frequency comparison for a load of 1000 lbf	49
5.9.	Vibration amplitude spectrum for a load of 1000 lbf.....	50
5.10.	Vibration amplitude spectrum for a load of 1500 lbf.....	51
5.11.	Mode shape and frequency comparison for the load of 2000 lbf	52
5.12.	Vibration amplitude spectrum – 2000 lbf.....	53
5.13.	FFT Plots and Extracted Experimental Resonance Frequencies	54
5.14.	Variation of natural frequencies with load level	55

LIST OF TABLES

TABLE	PAGE
3.1. Plate Dimensions.....	20
3.2. Material properties	20
3.3. Boundary condition along the four edges.....	22
4.1. Classical solution for natural frequencies (Hz) of unbuckled plate.....	30
5.1. Experimental resonance frequencies for different load levels.....	53

LIST OF SYMBOLS

#	Number
a	Length
ANSYS	Engineering analysis system
b	Width
Comp.	Compressive
D	Flexural rigidity
E	Young's modulus
EXP.	Experiment
f	Cyclic frequency in Hz
FEA	Finite element analysis
FEM	Finite element method
h	Thickness
Hz	Hertz
In	Inch
K_s	Shear buckling coefficient
lb	Mass unit
lbf	Force unit
MATLAB	Computer programming software
PC	Personal computer
P_{cr}	Critical buckling load

$P_{cr,c}$	Critical compressive buckling load
$P_{cr,s}$	Critical shear buckling load
PZT	Piezoelectric
ROT_x	Rotational degree of freedom in x-direction
ROT_y	Rotational degree of freedom in y-direction
ROT_z	Rotational degree of freedom in z-direction
s	Second
SHM	Structural health monitoring
t	Time
USCS	United States Customary System
U_x	Translation degree of freedom in x-direction
U_y	Translation degree of freedom in y-direction
U_z	Translation degree of freedom in z-direction
$\lambda_{m,n}$	Frequency parameter
ρ	Density
τ_{cr}	Critical shear stress
ν	Poisson's ratio
ω	Circular frequency in radian

CHAPTER 1

INTRODUCTION

1.1. Structural Health Monitoring

Structural Health Monitoring (SHM) techniques are useful for monitoring the condition of a structure during its operation, detecting damage, and warning if the margin of failure reaches an unacceptably low value. Availability of SHM techniques can help in the design and operation of structurally efficient, affordable, durable, and more reliable structures. As greater structural efficiency is sought, complex new designs are being examined. However, there is always the possibility of unforeseen failure modes with such new approaches. Often there is less margin of safety in newer designs. The availability of a reliable structural health monitoring technique can reduce the risk associated with deploying complex new designs into service. In addition, such monitoring techniques can provide valuable feedback to improve the design.

The structural health monitoring techniques employed in the past relied on sensing vibration, strain, thermal emissions, stress wave propagation, acoustic emissions, chemical species, or electrical conductivity to provide the necessary information. The benefits of this technology in the areas of aerospace, marine, civil infrastructure, and wind energy are obvious (Chang 2010). Over the past two decades, the SHM community has focused a great deal of attention on detecting the onset and growth of structural damage. Most of these analyses have been focused on detecting the onset and growth of inelastic damage in materials. The damage may be in the form of fatigue cracks in metals or fiber breakage and

matrix damage in composite materials. Other types of damage include corrosion and wear of structural materials. Such material degradations do grow and lead to catastrophic failures, if left unchecked. In addition to the structural health monitoring techniques, traditional nondestructive testing techniques have a long history of development and are widely used for the periodic inspection of life critical structural members for detecting the above types of material damage.

Some engineering structures are designed using thin members such as plates, beams, and columns. Such combinations result in weight and cost reduction, greater fuel efficiency and reduced environmental impact. However, structures made of thin walled members are susceptible to buckling. Structural instability caused by either design errors or by other factors can lead to catastrophic failures just as fatigue cracks and other types of damage do. However, there seems to be few structural health monitoring techniques specifically developed to detect the onset of buckling and to indicate the extent of postbuckling deformation in structural members.

New developments in high strength materials including carbon fiber composites have enabled the design of thinner structures. Reducing the thickness of the structural members can lower the buckling strength below the point at which the structure is likely to fail due to crack growth or plastic deformation. In fact, aircraft designers are actively considering the use of composite materials for primary structures operating in the postbuckling region (Falzon and Aliabadi, 2008).

1.2. Buckling Instability in Structural Elements

Structural instability is a condition that develops in structural members as a result of excessive load, which does not get categorized in the same class as other types of damage. The deformation that leads to the final catastrophic instability gradually grows in a structure as the load is increased in a manner similar to damage growth under statically applied load. However, this condition can be a precursor to structural failure just like other damage types.

Many catastrophic failures including those of multistory buildings (Sunder 2008), bridges (Akesson 2007), oil platforms, and aircrafts (Singer 2002) were attributed to unchecked growth of buckling deformation. Buckling can occur under compressive, bending, or shear loads. Depending on the loads, geometry, and boundary conditions, the initial buckling load may or may not be close to the ultimate load carrying capacity of the structure. For assuring safety and reliability of these structures, techniques for detecting the onset of structural instability are highly desirable. Failure due to buckling in some cases may be avoided with techniques capable of detecting the onset of instability and employing timely corrective measures. An example of such a possibility is in the operation of wind turbines. Wind turbine blades can experience local buckling under very high wind loads and if such incipient buckling is detected in a timely manner, it is feasible to rotate the blades out of wind direction and prevent damage.

Because of the catastrophic nature of buckling failure, most design practices employ very conservative approaches to determine design load levels. The actual buckling behavior of

individual members can widely vary, but there are many structures which exhibit regions of stable elastic postbuckled deformation (Kling 2008).

1.3. Regions of Postbuckling Deformation

The different regions of the load versus displacement of structural elements could be divided into elastic prebuckling region, elastic postbuckling region, and inelastic postbuckling region (Falzon 2008). The postbuckled deformation can be predominantly related to geometrical nonlinearities. Nonlinearities caused by material degradation usually do not set in until later. As illustrated in Figure 1.1, such structures may have significant load carrying capacity beyond the initial onset of buckling indicated by point A. It may be feasible to take advantage of this capacity if the deformation behavior is fully understood and if SHM techniques for reliable measurement of the margin before the onset of material damage at load B are available.

The nature of buckling process depends on the type of structural element, boundary conditions, loads, and the material. Hence the load range for the three regions, namely, the elastic prebuckling region, elastic postbuckling region, and the inelastic postbuckling region can vary significantly for different structural elements. In addition, in many structures there can be distinct local as well as global buckling modes. Buckling deformation can be magnified by in service material damage from other causes such as impact. For structures exhibiting a large postbuckling range, structural health monitoring techniques such as the one proposed in this dissertation is likely to be useful for first detecting the onset of buckling deformation. Further, if such structures are deployed to

operate beyond their prebuckling load range well into their elastic postbuckling range, the techniques proposed may be helpful in remotely detecting and quantifying the extent of postbuckling deformation and assessing the risk of catastrophic failure.

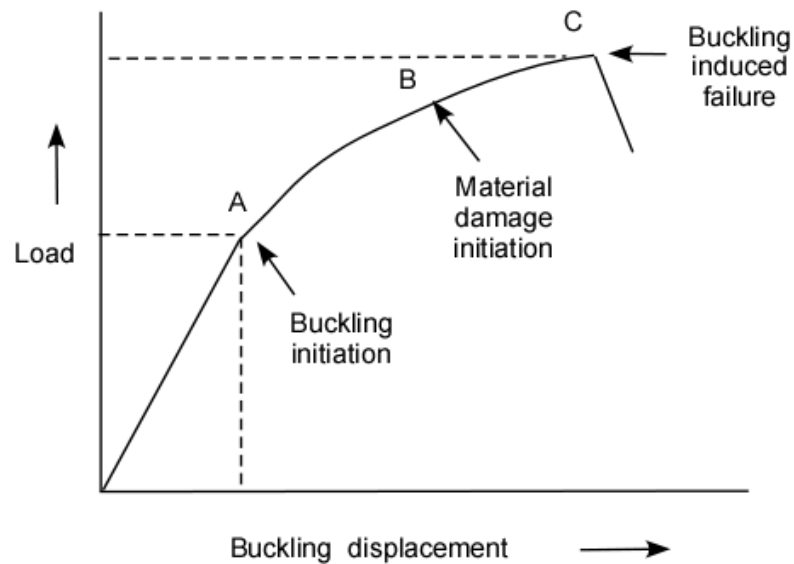


Figure 1.1. Schematic illustration of deformation and stability in post buckled region of structures

A square thin aluminum panel undergoing a stable elastic postbuckling deformation is chosen for developing this technique, with the hope that similar approaches may be applicable for other types of structural members undergoing instability. The onset of buckling and the postbuckled deformation characteristics of shear panels are of significant interest in a number of applications. Shear panels are found commonly in aerospace structures, buildings, and bridges.

Because of the advances in the vibration related instrumentation and wireless sensors, measurement of vibration response of structural elements in the field has become inexpensive and reliable. Hence, if vibration characteristics can be shown to be reliable indicator of the level of elastic postbuckling deformation, the technique is likely to be useful for field applications.

1.4. Objectives and Scope of the Dissertation

The objective of this dissertation is to develop a vibration based structural health monitoring technique capable of indicating the level of buckling deformation of a structural member while it is in service. In order to develop this technique the nonlinear elastic postbuckling deformation is first created in a square aluminum shear panel. This was done by both numerically using finite element technique and experimentally using appropriate loading conditions.

The vibration response of the shear panel including the natural frequencies and mode shapes at different points in the elastic postbuckling range are determined through numerical analysis as well as experiments. Changes in the natural frequencies and mode shapes from numerical and experimental analyses are examined. The sensitivity of vibration characteristics in monitoring the change in the shape of the shear panel is assessed.

1.5. Organization of the Dissertation

This dissertation is organized as follows: Chapter 2 first presents the literature related to both the analysis of the buckling related deformation in structural elements paying particular attention on shear panels. This is followed by review of the literature related to vibration analysis of buckled bars and plates and available structural health monitoring techniques for monitoring the extent of buckling. Chapter 3 describes the shear panel that was analyzed in this dissertation. Details of the finite element analysis for determining the transverse deflection of the panel at different load levels are presented. Further, the vibration analysis of the buckled panel at different points in the elastic postbuckling region is also presented. Chapter 4 describes the experimental work, including test fixture, experimental setup, procedure, and experimental results. The results include the transverse displacement profile of the shear panel at different load levels, the natural frequencies, and modes shapes corresponding to each of these load levels. The numerical results obtained in Chapter 3 are compared with the experimental results. The ability of the vibration based technique in determining the location of a given structural element in the elastic postbuckling region is evaluated. Chapter 5 provides a summary of the work performed and major conclusions.

CHAPTER 2

LITERATURE REVIEW

2.1. Introduction

The literature review in this chapter is divided into two sections. The first section is related to the buckling instability in structural elements including the buckling of shear panels. In this section, available literature related to both classical techniques as well as numerical analysis techniques for determining the onset of buckling and the extent of transverse deformation of the structure due in the postbuckled configurations are reviewed. The second section examines available structural health monitoring techniques for detecting buckling instability and then focuses on vibration analysis of bars, plates, and frames in their postbuckled configurations.

2.2. Analysis of Buckling Instability

Extensive literature on the buckling instability of structures is available. Several books are devoted to this important failure mechanism. Early books, such as Timoshenko (1985) and Thompson (1984), were devoted mostly to classical closed form solutions of plates, shells, and frames. In general the emphasis in the early research was on detecting the initial onset of instability. More recent books, such as Bazant (1991), present results related to postbuckling behavior including plasticity, visco-elasticity, creep, and local material instabilities. Galambos (1998) provides a compilation of theoretical and experimental results from the literature on the buckling instability of a variety structural elements as well

as assemblies of elements, mostly related to buildings and bridges. Simites and Hodges (2006) have compiled analyses related to both instabilities associated with structural members under static loading as well those operating in dynamic environments such as rotating shafts. A very extensive compilation of available experimental results on the buckling of bars, frames, plates, and shells have been presented in two volumes by Singer and his coworkers (1998 and 2002).

The structural element that is examined in this dissertation is a clamped square panel under edge shear at different levels of post-buckling deformation. Such an element is widely used in civil engineering structures as well as in aircraft structures. The post-buckling behavior of such an element has been extensively studied. In most applications, involve thin walled structures, such a shear panel is supported at the four edges by relatively rigid frames. Those rigid frames are assumed to transfer uniform shear stresses to the panel along the panel's four edges, and this assumption is true in the prebuckling state.

The post-buckled deformation behavior is governed, to a large extent, by the thickness-to-length ratio of the plate. In the pre-buckled state, the pure shear loading on the panel is equivalent to tensile load along one diagonal axis while the other diagonal axis is subjected to compressive load. The ability to support compressive load along one of the diagonals depends on the thickness-to-length ratio. Plates that are thick are able to support compressive forces along this diagonal, and hence the assumption of uniform shear along the edges of the square plate continues to be valid or partially valid for thick plates. Such plates are commonly used as shear walls in buildings and shear webs in bridges. However,

for very thin plates that are usually used in aircraft structures, the ability to support diagonal compression rapidly diminishes as a result of large transverse deflection of the panel. Available analytical and experimental studies on the postbuckling behavior of shear panels are reviewed in detail by Singer, et. al (Singer, 1998) and Galambos (Galambos, 1999). They also provide detailed description of the behavior of the shear panel and design approaches used in the industry. The buckling deformation in the square plate starts with a single elliptical bulge extending over much of the panel surface. As the shear stress is increased, the deformation develops into a series of elongated ellipses or folds with their major axis oriented along the diagonal carrying tensile stresses.

Basler and his coworkers (Basler, 1959 and 1963) investigated the behavior of relatively thick shear panels used in highway bridges. They undertook extensive experimental work and generated design rules for such structures. Basler considered the influence of plastic deformation and strain hardening in the postbuckling deformation in the web of such beams. Shear panels are also used as a primary means of energy absorption medium against seismic loading in high rise buildings. Refinements to the diagonal tension field model were suggested by a number of authors (Galambos, 1998). The cyclic deformation and collapse of shear walls, usually encountered as a result of earthquakes, was studied by Roberts (Roberts, 1991). Lubell (Lubell, 2000) determined the postbuckling behavior of shear wall in a scaled model of multistoried building using experiments and numerical analysis. Based on his findings Lubell provided an assessment of current design practice. Sabouri-Ghomi (Sabouri-Ghomi, 2005) considers the cyclic buckling behavior of stiffened and un-stiffened shear panels of various plate thicknesses.

He also considers the interactions between the framing system and the shear panels and the hysteretic behavior of the shear panel. Akesson's (Akesson, 2007) recent book provides a detailed analysis of the collapse of a number of bridges due to buckling.

Shear panels are of significant interest since the cyclic deformation in shear panels is a source of substantial energy absorption and vibration suppression when structures are subjected to seismic loading. The influence of geometrical and material nonlinearities on the deformation behavior and load carrying capacity panels of variety of thicknesses and boundary conditions has been studied using finite element technique by Alinia and coworkers (Alinia, 2008, 2009a, and 2009b). A detailed description of the three regions of buckling, namely, the elastic prebuckling region, elastic postbuckling region, and elasto-plastic postbuckling region, for the different types of panels. In particular their research provide information on the intermediate limit state at which the first occurs and the nature of plastic zone growth.

The buckling characteristics specific to the web of steel beams used in bridges are studied by Keerthan and Mahendran (Keerthan, 2010). They consider a new type of steel beam with hollow web sections to provide increased torsional rigidity. Their predictions compared favorably with experimental results for this type of construction. Hermann and his coworkers (Hermann, 2005) studied the postbuckling behavior of the spar web of a composite wind turbine blade using both finite element analysis and experiments. They found good agreement between the results of the finite element analysis and the experimental results and found that for this configuration, the spar web had a postbuckling reserve of 100% of its prebuckling strength.

The initial study of very thin plates under edge shear is attributed to Wagner (Wagner, 1931). In such cases, the compressive force across one of the diagonals is completely discounted and the plate is assumed to resist shear buckling solely from the tensile stresses across the other diagonal. In a recent text book on aircraft structures, Megon (Megon, 2010) describes this approximation commonly known as “diagonal tension theory.” This approximation is widely used in aircraft structural design.

While the ability of structural members to carry load in excess of their initial buckling load has long been recognized and partially utilized in aircraft constructions, the postbuckling behavior of structures, especially in the presence of complex interactions of material anisotropy and material and geometrical nonlinearities, is yet to be fully understood. There is renewed interest in exploiting the postbuckled reserve of structures to reduce the weight of aircraft structures, as illustrated by the compilation by Falzon and Aliabadi (Falzon, 2008). Numerical and experimental results for a composite stiffened panel under compression, reported by Kling, (Kling, 2008), illustrates the possibility of substantial weight reduction in aircraft structures if the postbuckled reserve of thin walled members could be safely exploited.

Advanced numerical analysis and experimental validations can help in the understanding of the postbuckling behavior of thin walled structures and their design. However, for the safe operation of structures in the postbuckling regime, there is a need for a means of assuring that the margin of safety of individual structures is maintained. Very few results related to determining in real time the progression of buckling deformation seem to be available in the literature.

2.3. Vibration of Plates and Shells

In the present dissertation, the changes in the vibration frequencies and mode shapes are used as indicators of the extent of buckling related deformation. Well known reports by Leissa (Leissa, 1969 and 1973) have compiled the vibration characteristics of plates and shells. A recent book by Soedel (Soedel, 2004) provides a review of more recent literature on vibration of plates and shells. However, the geometrical progression of a structure undergoing buckling deformation does not conform to the shapes of common geometries for which the vibration characteristics are available from the literature and additional information in this area is needed.

2.4. Vibration of Postbuckled Bars, Beams, and Plates

Eiseley and Luessen (Eiseley, 1963) consider the flutter of thin plates in both unbuckled configuration as well as buckled configurations. Eiseley (Eiseley, 1964) also provides a solution based on Ritz-Galerkin technique for the vibration of buckled beams and rectangular plates. He considers both free as well as forced vibrations. The shift in the frequency of beams fabricated by silicon micro-fabrication technology under externally applied buckling load is widely used for sensing various parameters. Such micro-resonators can be used for measuring pressure, force, mass flow, temperature, and acceleration. Tilmans et. al., (Tilmans, 1992) provide a thorough review of literature published till 1991, related to this sensor.

Nonlinear forced vibration of buckled beams are examined by Emam and Nayfeh (Emam, 2004). Emam and Nayfeh (Emam, 2009) provide solutions for the postbuckled

free vibrations of composite beams. They found that as the axial force on the beam increases the fundamental natural frequency of the beam gradually decreases and reaches a value of zero when the load reaches critical buckling load. Further increase in the axial load results in the increase in the natural frequency from this zero value.

The vibration response of postbuckled composite plates subjected thermal loading was examined by Lee and Lee (Lee, 1997). The variation of first, second, and third natural frequencies for the composite plate followed a trend similar to those reported by Emam and Nayfeh (Emam, 2009). As the thermal load increased the order of the first and second mode was found to be interchanged. Murphy and coworkers (Murphy, 1996a, 1996b, and 1997) studied the vibration characteristics of a clamped rectangular plate undergoing buckling under thermal stresses using analytical as well as experimental techniques. There was good agreement between the results generated by the two approaches. They found that the plate appeared to stiffen with respect to vibration response as it buckled. They also saw the crossing of modes in terms of frequencies. Similar tendencies were seen in the analysis of postbuckled laminated plates by Shiau and Chen (Shiau, 1997). Shiau used higher order plate theory with von Karman large deformation assumptions. Ilanko (Ilanko, 2002) used multi-term Galerkin's technique for determining the vibration characteristics of buckled rectangular plates, and obtained qualitatively same results as the earlier authors. Kundu and Han (Kundu, 2009) performed a similar analysis for a doubly curved laminated shell which underwent buckling deformation.

The postbuckling dynamics of rectangular plates including vibrations, bifurcation, and snapping were studied by Chen and coworkers using asymptotic finite element

technique (Chen, 2006a, and 2006b). Chen and Ro (Chen, 2010) studied using theoretical and experimental approach the vibration of a buckled elastic strip under axial displacement. While the buckling deformation of structural elements listed in this section of the review are amenable to analytical approaches, not all elements fall into this category. In general structural elements are likely to take complex shapes when they undergo buckling deformation, and the shear panel appears to be one such element. The vibration characteristics of such members do not seem to have been examined in the literature.

Available techniques for analyzing the vibration behavior of structures in their postbuckled state are compiled in a book by Virgin (Virgin, 2007). This book discusses the various engineering structures for which the vibration characteristics in the postbuckled state are of significant interest. In addition, both experimental as well as numerical approaches for analyzing the responses of various structural elements are also discussed.

2.5. Structural Health Monitoring Techniques for Detecting the Onset of Buckling

Vibration based techniques were among the first ones to be considered for monitoring the health of both civil and aircraft structures and an extensive literature on this subject is available. There has been several state of the art reviews on this topic. Becker et. al., (Becker, 2005) have assessed the role of smart structures in future aircraft systems that include the role of structural health monitoring, actuators, adaptive shape and load control and vibration suppression. They also examined the dynamic load and stability of aircrafts which is relevant to the topic of the current dissertation. Taha, et. al., (Taha, 2006) have compiled signal processing techniques specifically for damage identification in different

classes of engineering structures using wavelet transform techniques. Hsieh, et. al., (Hsieh, 2006) have reviewed techniques that are based on measuring changes in the frequencies, mode shapes, and modal damping values to detect changes in stiffness and damage development. They have included several examples of vibration based structural health monitoring techniques.

Fiber optic sensors are becoming affordable and multifunctional. They also have the important advantage in that they are embedded in structural members especially made of composite materials. Wild and Hinckley (Wild, 2008) have provided a state-of-the-art of techniques for vibration and other SHM techniques based on fiber optic sensing. They review the different types of fiber optic sensing techniques and discuss future possibilities of this very powerful sensing technique.

Wind turbine blades are among the largest composite structural elements constructed in large numbers and the reliability and performance of the blades are of societal importance. Several health monitoring techniques have been proposed for monitoring damage development in wind turbine blades. Ciang, Lee and Bang (Ciang, 2008) provide a comprehensive literature review of structural health monitoring techniques developed for wind turbine blades. Techniques based on the measurement of vibration and acoustic emission has been developed for monitoring damage development in wind turbine Sundaesan et. al. (Sundaesan, 2002), Schulz et. al., 2006 (Schulz, 2006), and Kirikera, et. al. (Kirikera, 2008), and Asamene et. al. (Asamene, 2010).

Annamdas and Soh (Annamdas, 2010) provide a review of techniques based on the measurement of electromechanical impedance for damage detection. Electromechanical

impedance changes are indicators of changes in the stiffness of the structure, which can arise from material change or change in the geometry as in the case of buckling of structural members.

Damage development or geometrical changes in structural elements result in changes in resonant frequencies as well as the related modes. While the measurement of changes in frequencies is straightforward, tracking the changes in the mode shapes is much more involved and needs expert input. Rainieri and Fabbrocino, (Rainieri, 2010) have reviewed the recent developments in the area of automated modal identification. Fan and Qiao (Fan, 2011) have provided a comprehensive review of vibration based damage identification methods. The methods reviewed techniques based on frequency, mode shape, curvature, and methods that jointly consider mode shape and frequencies.

CHAPTER 3

NUMERICAL ANALYSIS OF POSTBUCKLED DEFORMATION

3.1. Introduction

In this chapter the results from the numerical analysis of the postbuckling deformation of shear panels are presented. The objective of this analysis is to detect the onset of buckling and to determine the deformed shape of the panel as it undergoes various levels of buckling. Changes in the vibration characteristics of the panel as a function of the level of buckling deformation will be used as an indication of the margin of safety against permanent material damage and ultimate collapse of the panel.

The deformation pattern progressively changes as the edge shear load on the panel is increased. Initially there is uniform shear deformation below the critical buckling load. After the critical buckling load, out-of-plane buckling deformation develops during which the load versus central displacement curve exhibits nonlinear behavior. In the beginning, this deformation is totally elastic and the nonlinearity exhibited by the load-versus-central-displacement curve is termed geometrical nonlinearity. Depending upon the structural details, this elastic region can extend to well over double the load levels corresponding to the critical buckling load determined by classical linear analysis. The panel can completely revert to its original undeformed shape when the shear load is brought back to zero value. After a certain stage, inelastic deformation sets in and spreads with the increase in load, and the contribution to the nonlinearity from inelastic deformation is termed material nonlinearity. In metallic materials, the inelastic deformation is due to yielding and plastic

flow while in composite materials there can be damage in the form of matrix cracks, delaminations, and fiber fractures under combined shear and bending stresses caused by excessive buckling.

The focus of this dissertation is to develop a structural health monitoring technique capable of indicating the magnitude of buckling deformation and the safety of the structure in the elastic postbuckled deformation region of the load versus displacement curve. Hence, the nonlinear finite element analysis that is reported in this chapter is confined to this elastic region. ANSYS finite element software, version 11, was used for the buckling analysis.

3.2. Classical Approach

During the buckling process seen in bars, frames, plates, and shells, transverse deflection at increasing rate occurs when the axial force is increased at a constant rate. The buckling is caused initially solely by geometric effects. If the buckling increases unchecked, it can lead to damage to the materials and ultimately collapse of the structure. Some structures have the capacity to sustain load levels which are four to ten times the load at which the initial buckling occurs, without material damage, because of the redistribution of stresses within the buckled structure when it undergoes large deformation. As mentioned before the postbuckling reserve is used to some extent in the aerospace and civil applications. However, unexpected interactions such as those between, aging of material, impact damage, aerodynamic forces, and buckling can lead to unexpected outcomes. Hence, in the interest of safe operation of structures and increasing the structural efficiency

it is desirable to be able to monitor the buckling deformation while the structure is in service. This includes the determination of load at which a given structural element enters initial buckling deformation, and monitoring the progression of buckling deformation beyond the initial buckling load. Classical plate theory was employed to determine the both the initial buckling load and natural frequencies of the shear panel. The dimensions of the plate as well the plate isotropic material properties are shown in Table 3.1 and Table 3.2 respectively.

Table 3.1. Plate Dimensions

Length (a)	15.625 in
Width (b)	15.625 in
Thickness (h)	0.04 in

Table 3.2. Material properties

Aluminum 2024-T3	
Young's Modulus (E)	10×10^6 lb/in ²
Density (ρ)	0.0975 lb/in ³
Poisson's Ratio (ν)	0.33

The initial buckling load for square panel under edge shear is available from text books on this subject (Timoshenko 1985, Reddy 1999 and 2004). Solutions are usually obtained by energy method.

The equation for critical stress of isotropic plates is defined in the equation,

$$\tau_{cr} = \frac{K_s \pi^2 E}{12(1 - \nu^2) \left(\frac{a}{h}\right)^2} \quad 3.1$$

where, the coefficient K_s turns out to be 14.58 for square plate under edge uniform edge shear stress.

3.3. Numerical Modeling

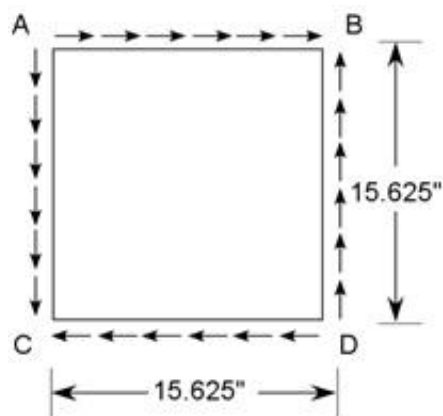
The finite element analysis of the plate was performed with progressively refined mesh sizes and the results were compared with classical buckling load. Finally a 125×125 elements finite element grid was used to model the buckling deformation. The edges of the panel were considered to be clamped, but the plate edges were free to move towards or away from each other as the buckling increases, as indicated by the boundary conditions listed in Table 3.3. Figure 3.1 shows the uniform shear load along the edges along with the equivalent corner loads on the panel with rigid boundaries. The results of this analysis will later be compared with experimental results in which the panel mounted on a rigid frame was loaded at the four corners along the vertical and horizontal diagonals.

The Shell 93 element from the ANSYS finite element library was used. This is an eight node element capable of modeling elastic and plastic deformation, as well as large strains. To induce buckling, a small transverse load was applied at the center of the plate. The nonlinear deformation of the shear panel was analyzed for corner loads up to 2000 lbf. Deformation patterns corresponding to several intermediate load levels at a spacing of 100 lbf were also determined. In addition, the initial buckling loads from this analysis were

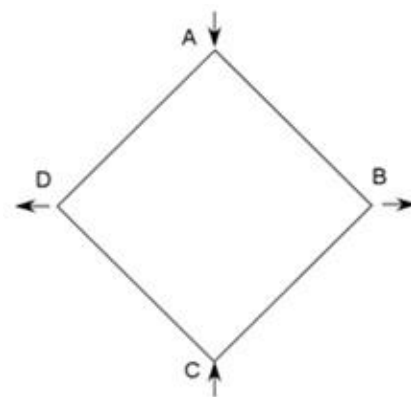
compared with the classical solution. As described later, the load-versus-displacement curve corresponding to the postbuckled deformation obtained from the present analysis was also compared with results from the literature.

Table 3.3. Boundary condition along the four edges

Clamped Boundary Condition						
Boundary	U_x	U_y	U_z	ROT_x	ROT_y	ROT_z
Bottom	1	1	1	1	1	0
Right	0	0	1	0	1	0
Top	0	0	1	1	0	0
Left	0	0	1	0	1	0
0 – Unconstrained 1 - Constrained						



(a)



(b)

Figure 3.1. Schematic of shear load application, (a) Edge shear, (b) Equivalent corner

As mentioned in Chapter 1, the load carrying capacity of the plate is divided into three different regimes, namely, (i) the linear elastic prebuckling regime, (ii) the nonlinear elastic postbuckling regime, and (iii) the nonlinear elastoplastic regime. It is the intention of this dissertation to confine itself to the nonlinear elastic postbuckling region. It is estimated that the linear elastic regime extends to only about 25% to 30% of the ultimate load carrying capacity of the shear panel. The nonlinear elastic regime is estimated to extend to about 70% to 75% of the ultimate load carrying capacity of the panel (Alinia (2008)). Based on these estimates, the maximum load applied along the diagonals was limited to 2000 lbf. The ability to utilize the postbuckling strength reserve of the panel before it enters permanent plastic deformation without risk can lead to cost and weight savings in many applications. The objective of this research is to develop vibration based structural health monitoring techniques capable of real-time indications of the extent of buckling deformation in such structural members.

3.4. Results of Numerical Analysis

3.4.1. Validation of the Numerical Results

The initial validation for the numerical technique is obtained first by comparing the trend seen in the load vs. transverse deformation obtained from finite element analysis with closed form solution for the shear panel. The deviation from the initial linear path in the load vs. displacement was seen at load level of 726 lbf. The same value was obtained from classical solution, which validates the current numerical analysis in the elastic prebuckling regime. However, no closed-form solutions are available for the large displacements in the

nonlinear elastic postbuckling regime. Hence, for validating the current numerical solution in the nonlinear region, results were generated for the plate dimensions used by Alinia (2008) for postbuckling analysis of shear panels. The plate dimensions used by Alinia were 39.37 in. x 39.39 in. x 0.118 in. (1000 mm x 1000mm x 3 mm), and the material was steel with Young's modulus of 30 000 ksi (206 GPa) and Poisson's ratio of 0.3. Figure 3.2 shows the comparison of the two results.

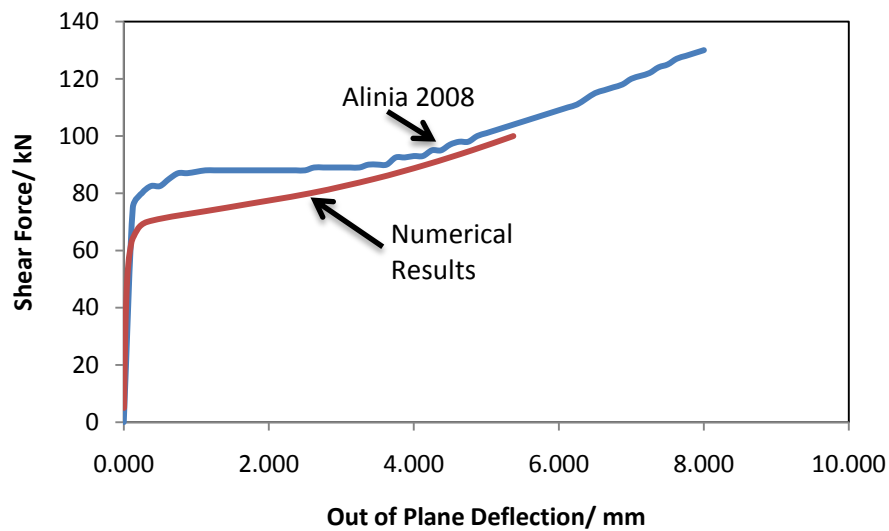


Figure 3.2. Comparison of the numerical techniques

The two graphs have some differences near the beginning of the nonlinear elastic regime, but the differences decrease as the deformation increases. Since the interest in this study was confined to elastic postbuckling region the numerical predictions was obtained only up to a maximum shear load of 1414 lbf. In Chapter 5, the numerical predictions will be compared with experimental results.

3.4.2. Results for the Aluminum Panel

The transverse deflection profiles for the plate under different levels of diagonal compression are shown in Figure 3.3. Initially, the buckling pattern corresponds to one elliptical bulge of the plate. At later stages, two additional bulges appear near the corner of the plate with displacements that are in the negative z direction relative to that of the central bulge. Further, the central elliptical bulge becomes narrower with the increase in load level. The deformation near the top corner is greater than the deformation near the bottom corner. Buckling patterns for this panel was also determined for loads up to 3000 lbf. The load-versus-central-displacement curve for the aluminum shear panel is shown in Figure 3.4. The maximum transverse deflection due to buckling occurred at the center of the plate throughout the buckling process for corner loads up to 2000 lbf. Just after the initial buckling load, there is a sudden increase in the slope of load versus deflection curve. Beyond the load of 1000 lbf the slope of the curve gradually decreases. The maximum central deflection of the panel at a load level of 2000 lbf was 0.178 inches, which is nearly five times the thickness of the panel. The complete deformed shape of the neutral axis of the plate was obtained in terms of nodal coordinates from the finite element analysis. This deformed shape of the plate was used to model the vibration characteristics of the plate in Chapter 4. The phenomenon of snap through buckling was seen at higher loads but they are not discussed further in this dissertation.

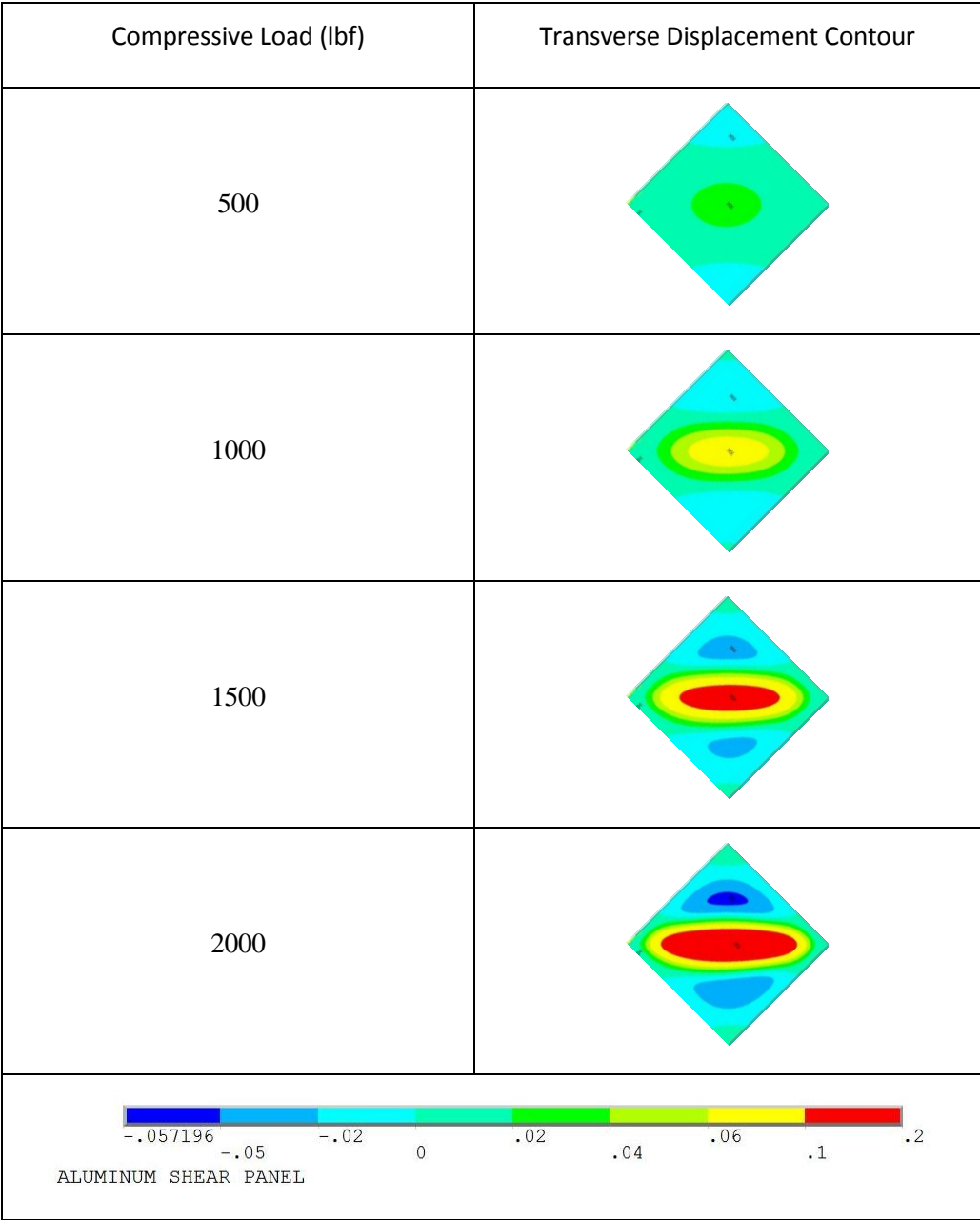


Figure 3.3. Nonlinear buckled plate contour

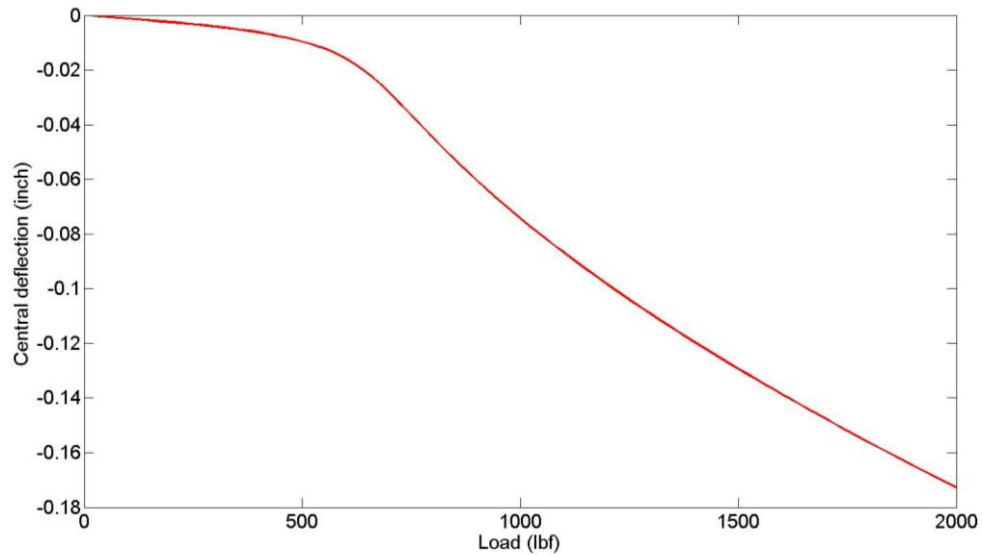


Figure 3.4. Numerical results of variation of transverse deflection with load

3.5. Summary

The objective of the numerical analysis described in this chapter was to determine the deformed shape of the shear panel as it undergoes different levels of buckling in the nonlinear elastic postbuckling regime. The panel considered was a square plate, $15.625'' \times 15.625''$ and with a thickness of $0.04''$ clamped along the edges. The panel was loaded by uniform shear along the four edges well into the postbuckling range. Geometrically nonlinear finite element technique was used for determining these shapes. First the numerical approach was validated by comparing with results available in the literature. The deformed shapes determined from this analysis will be used in the next chapter to determine the feasibility of a vibration-based structural health monitoring technique capable of indicating the margin of safety available against buckling induced collapse of the shear panel.

CHAPTER 4

NUMERICAL ANALYSIS OF THE VIBRATION CHARACTERISTICS OF THE SHEAR PANEL

4.1. Introduction

The objective of the work performed under this section is to determine the changes in vibration characteristics of the postbuckled panel as it undergoes different levels of buckling. It was anticipated that these changes in the resonant frequencies and mode shapes may be used as indicators of the state of the shear panel and the safety margin available against catastrophic collapse. The natural frequencies and mode shapes of flat plates and shells are well documented in the literature. However, when structural members undergo large displacements as a result of buckling, there is significant change in their geometry including their curvatures. Such shapes do not conform to regular shell geometries and very few results seem to be available regarding the dynamic characteristics of postbuckled structures. There is significant variation in the flexural stiffness of the shear panel as it undergoes postbuckled deformation, and these variations are expected to be reflected in corresponding variations in natural frequencies and mode shapes. Simple and inexpensive tools including wireless accelerometers are available to remotely monitor the frequency and amplitudes and mode shapes of vibration. Hence it is feasible to detect the onset of buckling and measure the postbuckling deformation if unambiguous relationship between buckling deformation and vibration characteristics could be established for widely used structural elements.

The solution for the natural frequency and mode shapes for the clamped square shear panel in its unbuckled form available from the literature (Leissa 1996) is given by

$$\omega_{m,n} = \frac{\lambda_{m,n}}{a^2} \sqrt{\frac{D}{\rho h}} \quad 4.1$$

where n and m indicate the nodal lines lying in the x - and the y -directions, respectively, including the boundaries as nodal lines, and

$$D = \frac{E h^3}{12(1 - \nu^2)} \quad 4.2$$

The frequency, $f_{m,n}$, is given in equation 4.3 and the solutions are given in Table 4.1.

$$f_{m,n} = \frac{\omega_{m,n}}{2\pi} \quad 4.3$$

4.2. Numerical Modeling

The model used the same plate geometry, boundary conditions, material properties, and finite element idealization as described in Chapter 3. The assumption used in the numerical modeling is that the vibration behavior of the buckled plate is the same as that of a curved plate with the curvature of its neutral axis matching the transverse deflection of the buckled plate. Therefore, at each buckling load level, the transverse deflections of the plate at all the nodes were extracted for further analysis. The extracted deformed shape was used in the vibration analysis with the plate edges under clamped conditions. The ANSYS vibration analysis package was used to determine the natural frequencies and mode shapes of the panel in its different states. The results presented are for small amplitude free vibrations of the panel under uniform edge shear load.

Table 4.1. Classical solution for natural frequencies (Hz) of unbuckled plate

m/n	1	2	3	4	5	6
1	56	115	206	329	482	668
2	115	169	257	379	531	715
3	206	257	343	462	614	796
4	329	379	462	579	729	911
5	482	531	614	729	877	1055
6	668	715	796	911	1055	1237

4.3. Results of the Dynamic Analysis

The natural frequencies and mode shapes of the shear panel in the prebuckled state were first obtained from the numerical analysis. These results were validated by comparing with classical solutions available in the literature (Leissa, 1964). The numerically derived results closely followed the predictions of the classical solution. The frequencies and mode shapes of the panel in the unloaded prebuckled state are shown in Figure 4.1 for the first 21 modes of vibration. The mode shapes of the panel in the prebuckled state have regularly spaced patterns. For each of the postbuckled states, including those at load levels of 1000 lbf, and 2000 lbf, the natural frequencies and mode shapes were determined. These results are shown in Figure 4.2 and Figure 4.3. In addition to the mode shapes and frequencies, the deformation pattern of the shear panel under the two different load levels are also shown in these figures. The changes in the mode shapes and frequencies may be related to the transverse deformation and corresponding geometrical changes as a result of buckling deformation at these respective load levels.

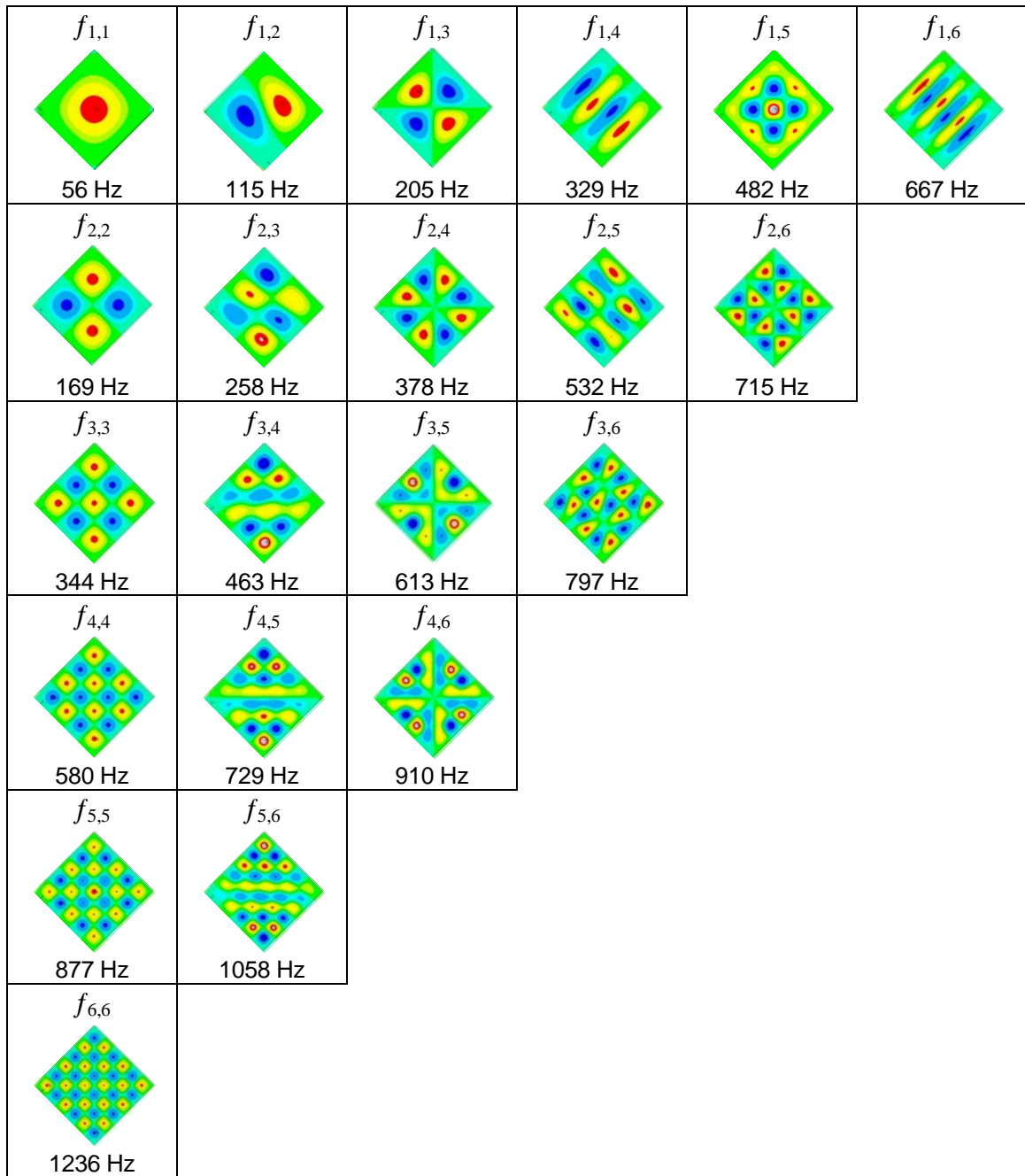


Figure 4.1. Mode shapes and frequencies of the prebuckled shear panel

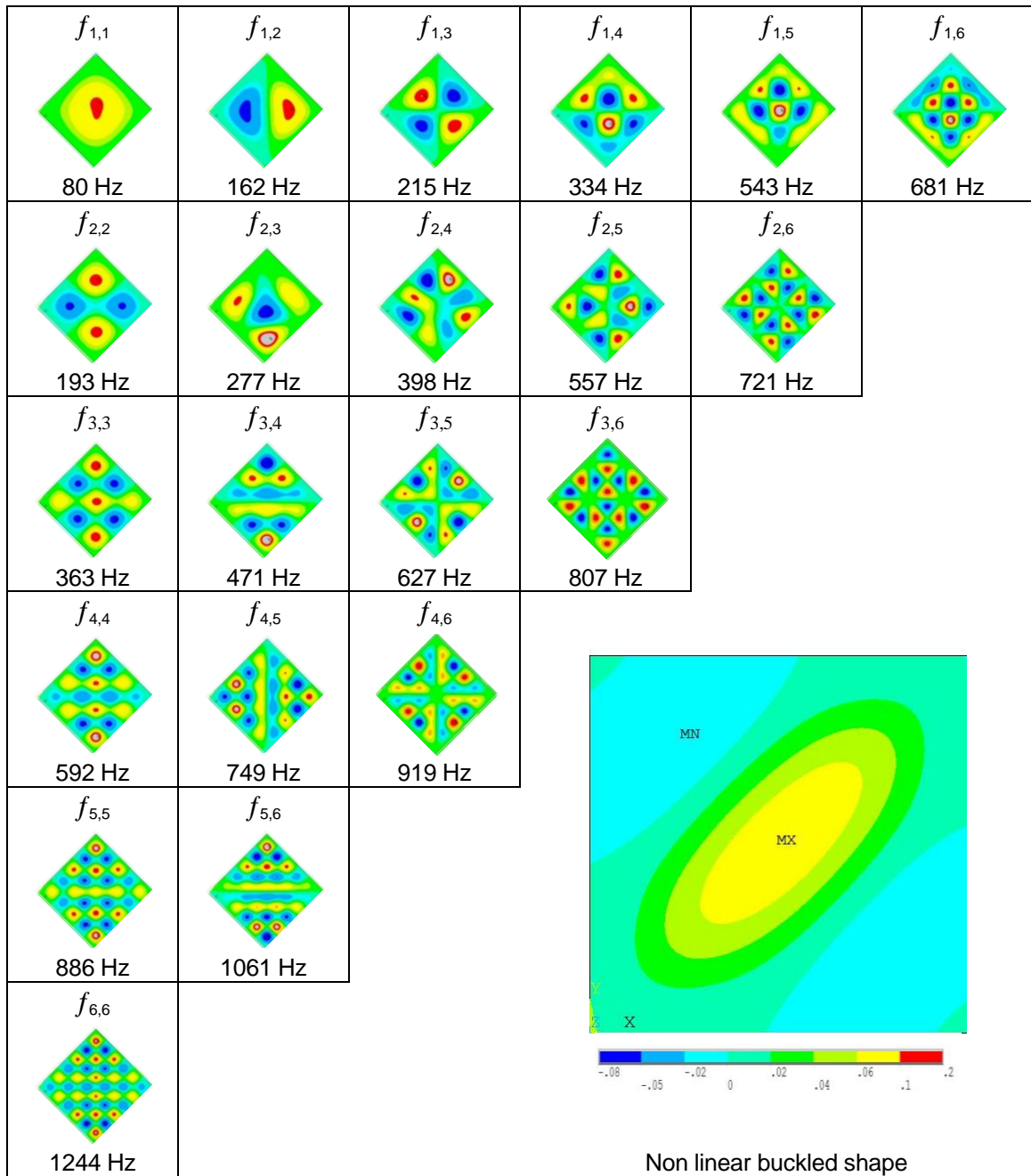


Figure 4.2. Natural frequencies and mode shapes of panel for the load of 1000 lbf

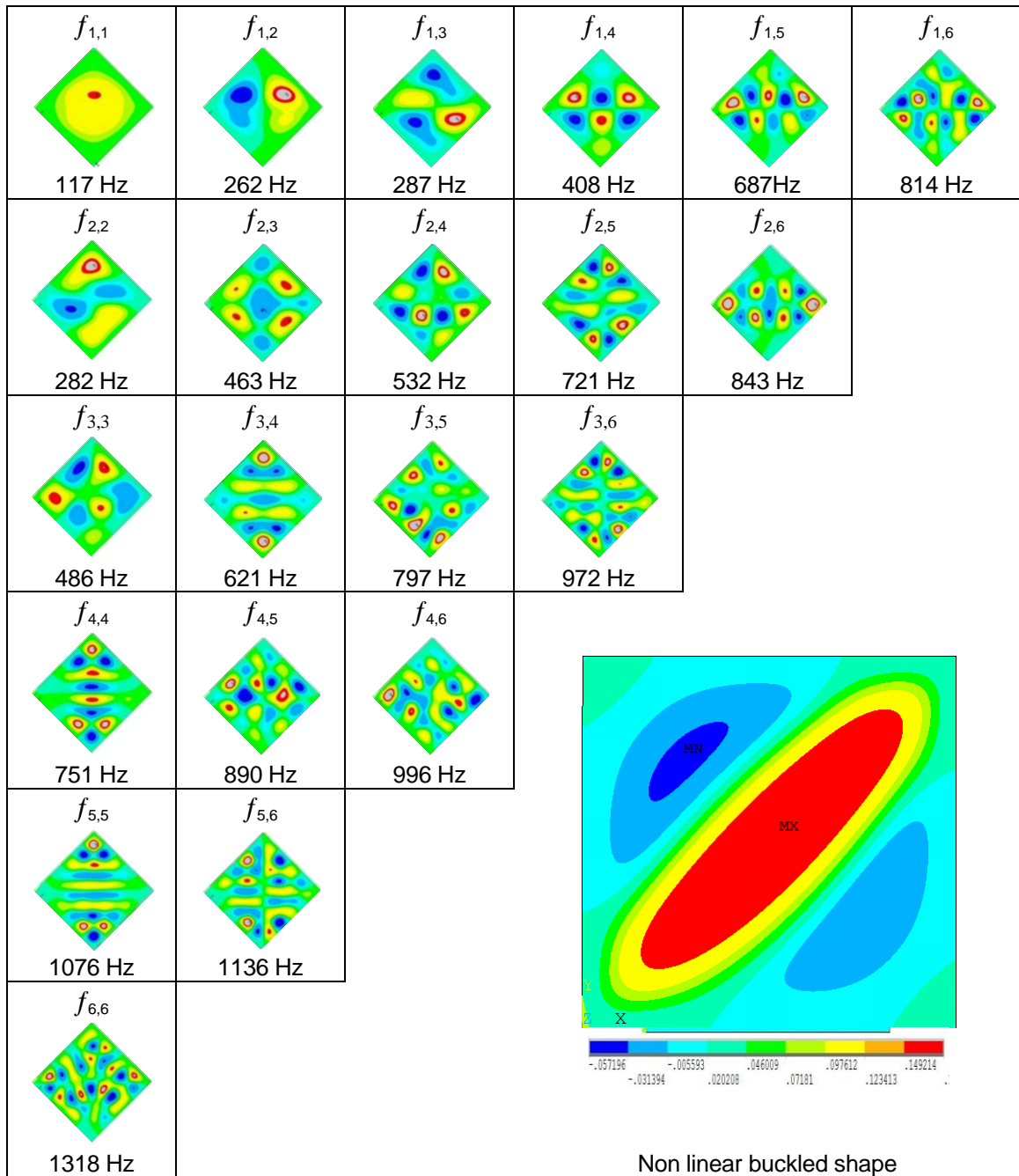


Figure 4.3. Natural frequencies and mode shapes of panel for the load of 2000 lbf

The first five mode shapes are regrouped and presented in Figure 4.4 for load levels of 0 lbf, 1000lbf, and 2000 lbf. The significant changes in the mode shape and the resonance frequencies are mainly due to the loading levels.

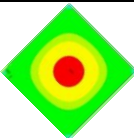
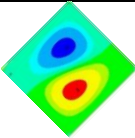
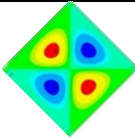
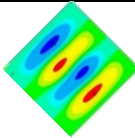
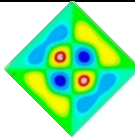

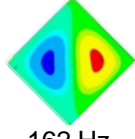
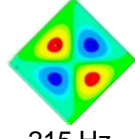
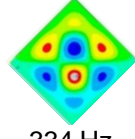
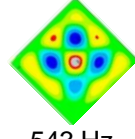
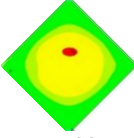
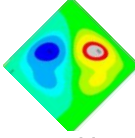
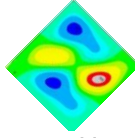
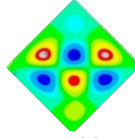
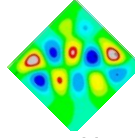
Load (lbf)	$f_{1,1}$	$f_{1,2}$	$f_{1,3}$	$f_{1,4}$	$f_{1,5}$
0	 56 Hz	 115 Hz	 205 Hz	 329 Hz	 483 Hz
1000	 80 Hz	 162 Hz	 215 Hz	 334 Hz	 543 Hz
2000	 117 Hz	 262 Hz	 287 Hz	 408 Hz	 687 Hz

Figure 4.4. Comparison of the first five frequencies and mode shapes of panel at different stages of buckling.

The variation of frequencies as a function of applied load is shown in Figure 4.5. The significant changes are seen in the natural frequencies at different stages of deformation. The changes in the frequencies and mode shapes as a result of buckling are clearly seen in this figure. The variation of the frequencies with the buckling load for modes $f_{1,1}$ to $f_{1,5}$ are plotted in Figure 4.5. The results from the numerical simulations suggest that the modes $f_{1,1}$ and $f_{1,2}$ are likely to be the most sensitive ones for detecting the onset of buckling for the square shear panel.

In the frequency $f_{m,n}$ the subscripts m and n respectively refer to the number of nodal lines along the two mutually perpendicular directions including the boundaries on nodal lines. The well known trend of increasing frequency with increase in the number of nodal peaks is seen among the different modes. Further, in the unbuckled state the nodal pattern across the two diagonals are interchangeable.

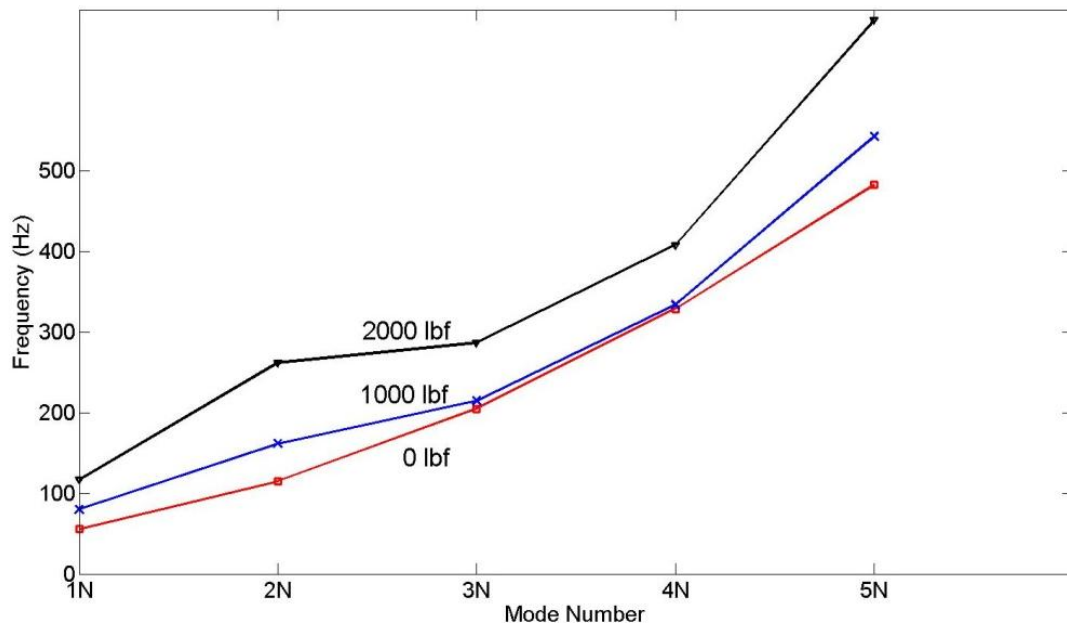


Figure 4.5. Variation of natural frequencies as a function of applied load

Distinct differences in the mode shapes as well as frequencies are seen as a result of the buckling displacements. The patterns along the two diagonals are no longer interchangeable. A consequence of this loss of interchangeability, the order of vibration modes are difficult to classify. For example $f_{2,3}$ in unbuckled condition is easily

recognizable. The vibration mode shape for buckled panel which is named as $f_{2,3}$ does not have equal number of nodal lines along the two opposite edges. The regions around the points of peak displacement and curvature seem to be affected most in terms of change in the vibration pattern.

Higher levels of buckling deformation at higher load level resulted in further increase in natural frequencies as well as distortion of the mode shapes. The largest percentage of change seems to be occurring for the modes $f_{1,1}$ and $f_{1,2}$. For a corner load of 1000 lbf the increase in the frequencies $f_{1,1}$ and $f_{1,2}$ respectively were 43% and 41%. For load level of 2000 lbf the increase in frequencies were 109% and 128% respectively. There were large distortions in the higher order modes as the buckling load was increased and hence were difficult to track. It was also difficult to obtain consistent changes in the frequencies of these modes.

4.4. Summary

Numerical analysis using finite element technique was performed to determine the dynamic characteristics of the shear panel in its different states of postbuckling deformation. The results for the panel in the unbuckled state were compared to the classical solutions. As expected, significant variations in the natural frequencies and mode shapes were observed as the shear panel undergoes moderate transverse static deflection due to buckling. The buckling deformation appears to progressively increase the apparent flexural stiffness of the panel, whose effects are seen in the gradual increase in the natural frequencies. There were also significant changes in the mode shapes as a result of the

buckling deformation. The maximum transverse static deflection due to buckling considered was 0.178 in. which occurred at the center of the plate. This deflection caused the frequencies $f_{1,1}$ and $f_{1,2}$ to increase by 43% and 41% respectively for a buckling load of 1000 lbf and by 109% and 128% for 2000 lbf load.

CHAPTER 5

EXPERIMENTAL DETERMINATION OF VIBRATION CHARACTERISTICS OF POSTBUCKLED SHEAR PANEL

5.1. Introduction

In this chapter, the experimental investigation of the vibration characteristics of the shear panel at different stages of buckling deformation is described. The panel was loaded using a test fixture in an MTS testing machine to simulate uniform edge shear. The transverse displacements due to buckling were measured using a dial gage. The natural frequencies and mode shapes were determined using a laser vibrometer. These experimental results are used to evaluate the numerical results and to assess the feasibility of vibration based structural health monitoring technique for real time determination of the margin of safety of structures operating in the postbuckling regime.

5.2. Experimental Setup

The material, specimen dimensions, and load levels used in the experimental work paralleled the values used in the numerical study. All four edges of the plate were clamped between two rigid steel members of the loading frame commonly referred to as a “photo-frame fixture” in the literature (Singer 1998). The photo-frame fixture used to load the specimen consisted of two square frames, one at each side of the specimen, with hinges at the four corners and bolted all around the frame as illustrated in Figure 5.1(a). This configuration allows the applied compressive force to transfer through the frame members

into the panel as edge shear as illustrated in Figure 5.1(b). To eliminate any deviation from the clamped boundary condition along the edges, thin rubber gaskets were used along the clamped edges. The corner pins were coated with molybdenum disulphide grease to allow the fixture to freely deform under the applied corner forces. The panel was clamped using sixteen $3/8^{\text{th}}$ inch diameter steel bolts.

The shear panel held in the fixture was loaded in a 20,000 lb capacity servo-hydraulic testing machine. The results reported correspond to compressive loads across the vertical diagonal. Six PZT patches ($0.787 \text{ in} \times 0.394 \text{ in} \times 0.02 \text{ in}$) are bonded on the back of the plate at different locations so that it is possible to excite the specimen in a range of frequencies and get vibration amplitudes for different modes as shown in Figure 5.1(c). A power amplifier is used to excite the PZT patches.

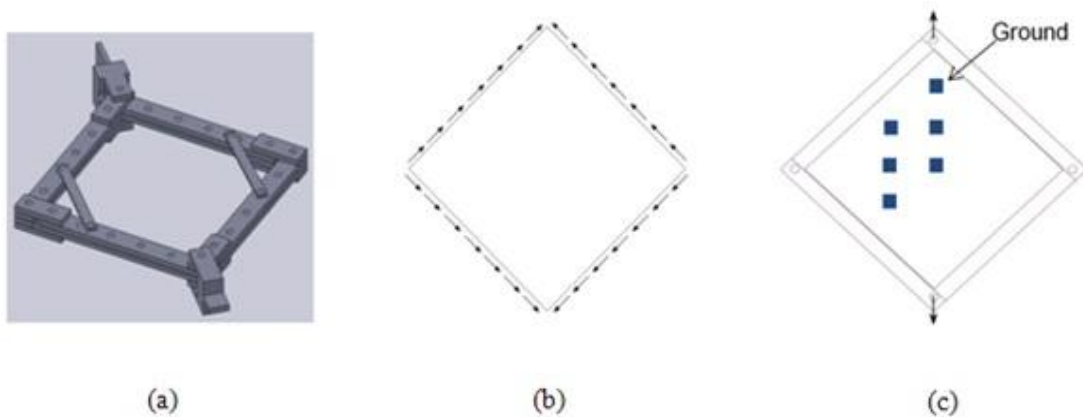


Figure 5.1. (a) Picture Frame Setup for Shear Loading (b) Effective edge shear (c) Location of the PZT patches for exciting vibration

A Polytec (PSV) OFV-200 multi-point scanning laser Vibrometer (Polytec, 2008) was used in this experiment to detect and record the characteristics of vibrations on the panel's surface with a helium-neon laser as seen in Figure 5.2. The front surface of the plate was divided into a sufficient number of measurement points for capturing vibration frequencies and mode shapes. Retro-reflecting tape was attached at each measurement point to obtain a sufficiently strong signal from the surface of the specimen.

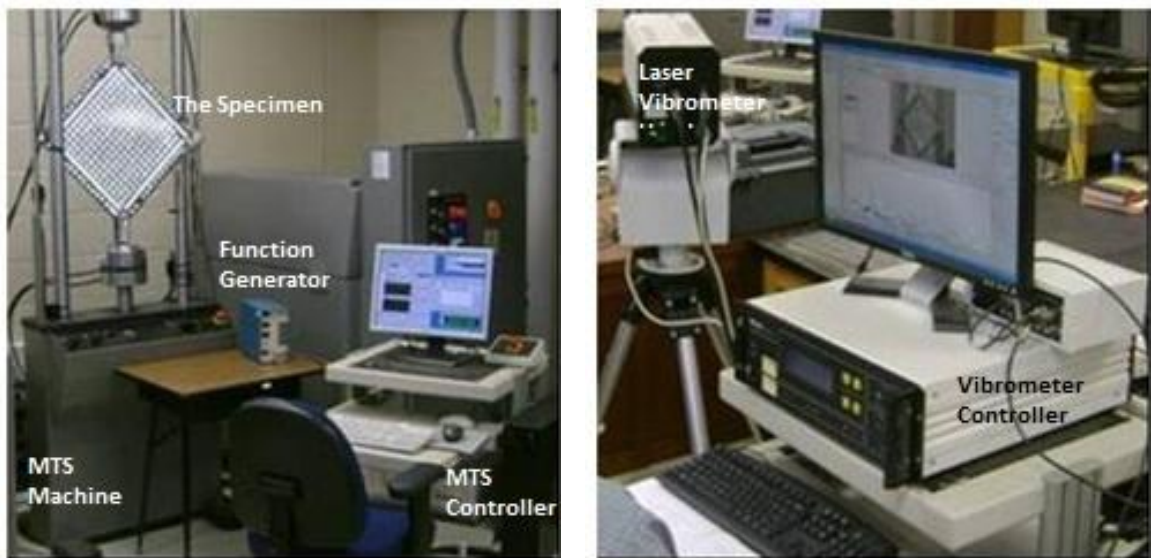


Figure 5.2. Experimental set-up

The function generator within the Vibrometer was used to generate the signal for exciting the shear panel. A frequency range of 30 Hz to 1000 Hz was initially chosen for these experiments. Initial trials used a uniform chirp excitation extending from 30 Hz to 1000 Hz. Most of the experiments were performed with such an excitation. As described

later, results from some of the tests were confirmed using pure sine wave excitations at selected frequencies. The Vibrometer repeatedly excites of the panel in the selected mode, and during each of the chirp excitations, the laser beam remains stationary at one spot on the panel where retro reflective tape is positioned. As the chirp excitation sweeps from 30 Hz to 1000 Hz the different resonant frequencies of the panel are excited. The Vibrometer measures the velocities corresponding to such resonant frequencies. Typically the chirp excitation lasts 5 to 10 seconds at a spot. The scanning of all the points on the surface is completed in about 60 minutes. The displacements corresponding to different frequencies at each point on the panel surface is stored in the Vibrometer. The velocities measured at all points on the surface are assembled by the Vibrometer to generate the panel's resonant frequencies and mode shapes.

The corner load on the panel was gradually increased to 2000 lbf. The buckling displacements and vibration characteristics were determined at intervals of 500 lbf. Three sets of experiments at these load levels after the panel was disassembled from the fixture to confirm the reproducibility of results. Based on initial trials, the frequency range 50 Hz to 1000 Hz was used in these measurements. It was confirmed that, for all the loads used here, the fundamental resonance frequencies were beyond 50 Hz. The panels were removed after these experiments from the frames and were found to recover their completely flat configurations in their unloaded condition. The data from the three tests indicated that the results remained substantially unchanged from one test to another. In the comparison between experimental and numerical results, the data from trial 2 was used. Experiments corresponding to trial 2 and trial 3 are done with all the instrumentation settings maintained

at the same condition in two different days. For trial 1 some of the instrument settings such as the resolution of the FFT were different. But these changes were not expected to affect the vibration characteristics of the plate. Nevertheless, all three trials confirm the repeatability of this experiment.

A dial gage was used to determine the static deflection at each load level at ten different locations on a quadrant of the panel's front surface. The locations were selected assuming the deflection is symmetric about both the horizontal and the vertical axes of the setup. For measuring the deflection at a given location the magnetic holder of the dial gage was clamped on the near side of the loading frame. With the dial gage fixed in this position, the load on the panel was gradually increased to record the deflections at 500, 1000, 1500, and 2000 lbf. The dial gage was then moved to a new location and the procedure was repeated. The accuracy of the deflection measurements was verified through independent measurements. The deflection of the cantilever arm holding the dial gage due to the force applied at the dial gage was found to be negligible. The static deflection of the entire surface was obtained making use of the symmetry of the plate deflection.

The resonance frequencies were identified with the aid of FFT plots obtained for the entire range of excited vibration frequencies. The resonance frequencies extracted for comparisons were selected so that the relevant mode is represented as a resonance state in all the selected load levels.

5.3. Results

5.3.1. Static Deflection in the Post Buckled Region

The magnitude of the transverse deflection (measured using the dial gage) at different levels of buckling load are plotted in Figure 5.3. The transverse deflections were measured at the corners of a grid with 1 inch spacing.

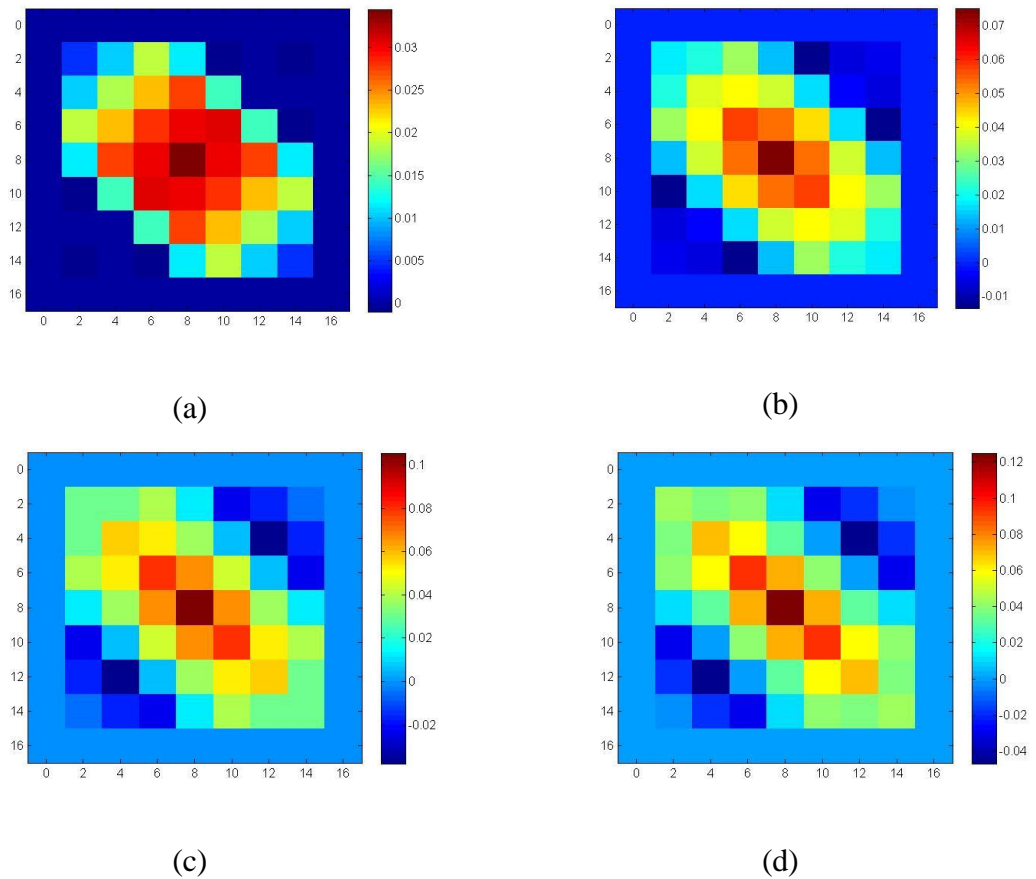


Figure 5.3. The transverse deflections of the postbuckled shear panel at different load levels (a) 500 lbf, (b) 1000 lbf, (c) 1500 lbf, and (d) 2000 lbf

Displacements were measured only for one quadrant of the panel since the deformation is assumed symmetric with respect to the vertical and horizontal diagonals. The resolution of the measurement is not comparable to the one obtained from the numerical solution. However, the elliptical shape of the transverse deflection contours can be recognized from the experimental results. In addition, the narrowing of the elliptical shape as the load is increased is also evident from these figures.

The variation of the central deflection of the panel with the applied load is shown in Figure 5.4. In this figure, the corresponding result from the numerical analysis from Chapter 3 is also included for comparison.

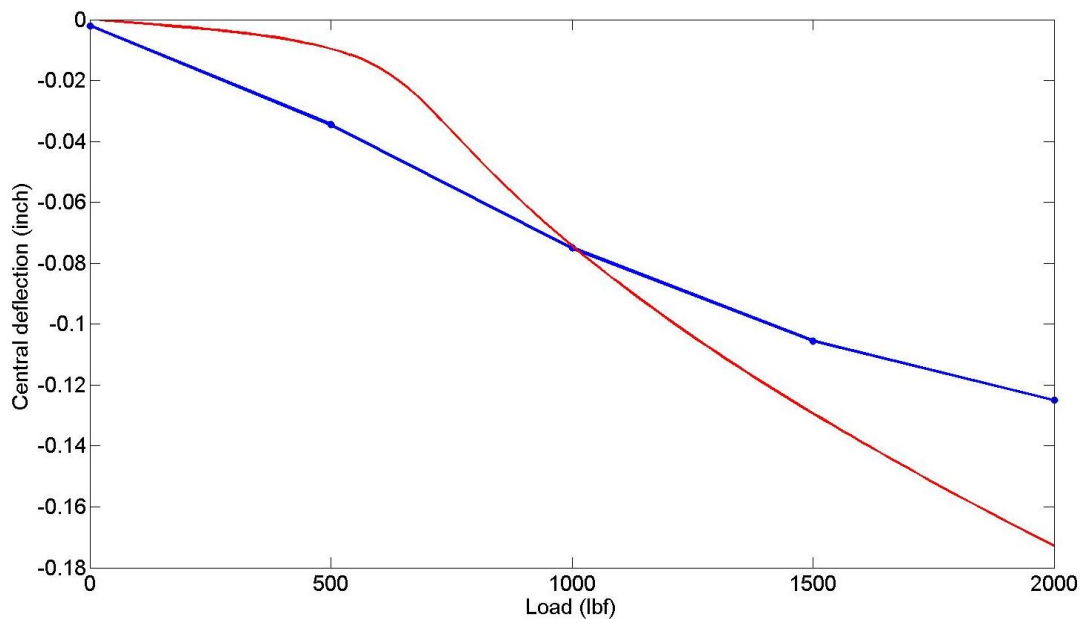


Figure 5.4. Variation of central deflection as a function of applied load

The results from the numerical analysis indicated a sudden change in the slope of the load vs. deflection curve around the initial buckling load. However, such a change was not present in the experimental results. The central displacement corresponding to one of the tests was different from the results shown in Figure 5.4, and the difference between those experimental results and the finite element simulations was larger.

5.3.2. Dynamic Characteristics in the Postbuckled Region

The vibration modes were easily excited when the plate was in its unbuckled condition. The amplitudes of oscillation were adequate and the modes shapes were clearly recognizable even when the excitation forces applied through the PZT elements were relatively small. However, when the plate was buckled, the amplitude of oscillations decreased and the mode shapes could not be clearly recognized. Hence to confirm that the mode shapes selected were correct, the resonant frequencies were first identified from chirp excitation of the shear panel. The scans were repeated with constant frequency sinusoidal excitation at each of the selected frequencies and the mode shapes were recorded. The mode shapes shown in this section were from such constant frequency sinusoidal excitations.

The vibration responses for modes $f_{1,1}$ to $f_{1,5}$ of the unloaded panel are shown in Figure 5.5. The results include the numerical predictions as well as the mode shapes determined from the three different experiments. Good agreement between the numerical and experimental results is seen in these results.

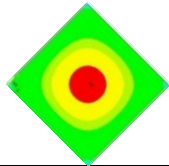
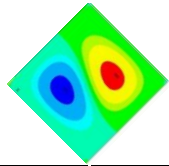
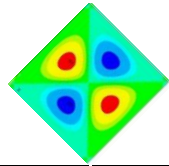
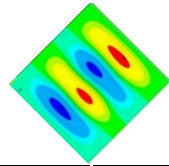
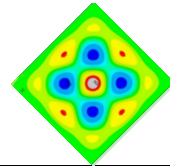
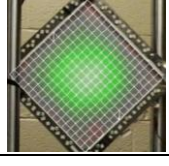

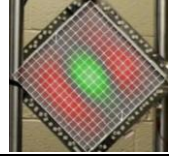
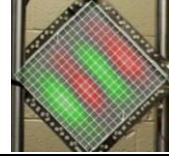
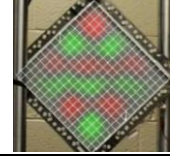

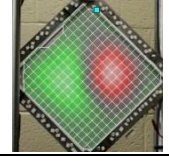
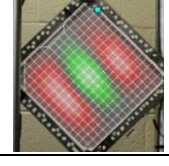
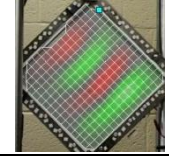


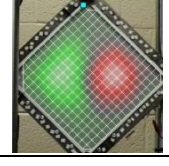
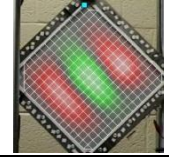

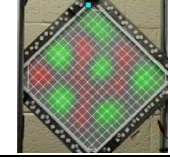
		$f_{1,1}$	$f_{1,2}$	$f_{1,3}$	$f_{1,4}$	$f_{1,5}$
FEA Mode shapes and frequencies						
		56 Hz	115 Hz	205 Hz	329 Hz	482 Hz
Experimental Mode shapes and frequencies	Trial #1					
		57 Hz	113 Hz	193 Hz	306 Hz	427 Hz
	Trial #2					
		59 Hz	116 Hz	199 Hz	306 Hz	451 Hz
	Trial #3					
		59 Hz	116 Hz	198 Hz	307 Hz	451 Hz

Figure 5.5. Mode shape and frequency comparison for free load conditions

Further, the results from the experiments were found to be fairly reproducible after the panel was disassembled from the fixture and reassembled. These results were listed as results from Trial 1, 2 and 3. The vibration amplitude spectrum corresponding to chirp excitation ranging from 50 Hz to 1000 Hz is shown in Figure 5.6. A large number of resonant frequencies are seen in this frequency range. Further, a number of pairs of modes with each mode within a pair having nearly same frequencies are seen in this figure. Such modes were found to be identical except that the second mode of the pair was rotated by 90 degree with respect to the first mode. Apparently, the small shift in the frequency is caused

by minor differences in the boundary conditions between the four edges of the panel. Even though efforts were made in the design of the loading fixture and assembling the fixture with uniform bolt torques, these differences persisted.

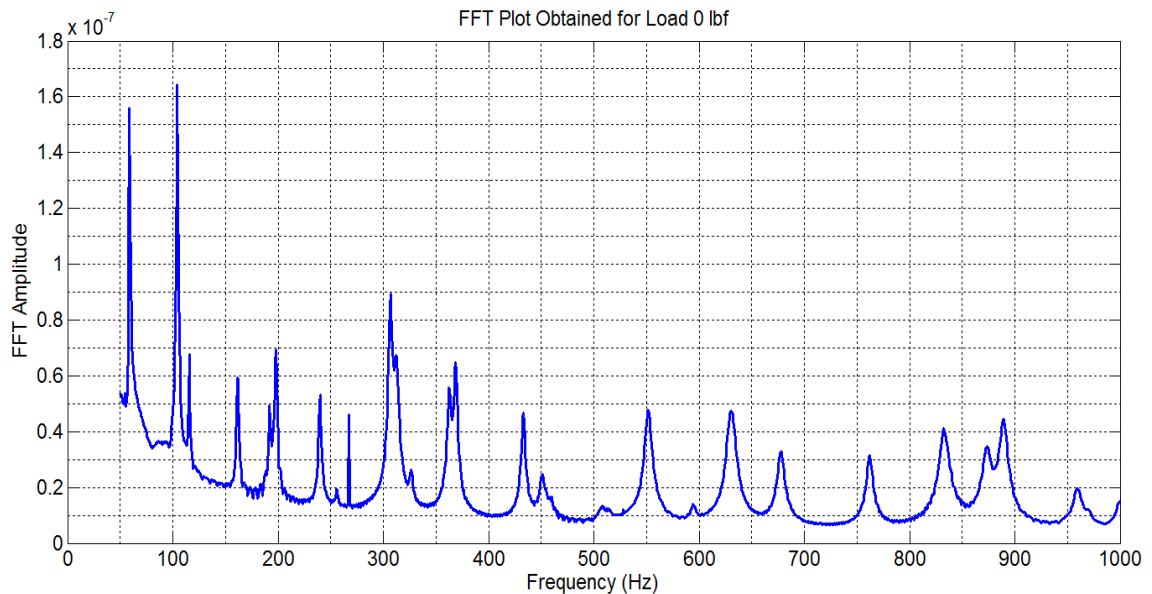


Figure 5.6. Vibration amplitude spectrum under no load condition

Vibration amplitudes for corresponding to a corner load of 500 lbf are shown in Figure 5.7. The frequencies of resonance are shifted relative to the unloaded condition. The pairs of modes which were adjacent to each other in the loaded condition seem to move away from each other, apparently caused by the elliptically shaped buckling deformation whose major axis is oriented along the horizontal diagonal of the shear panel.

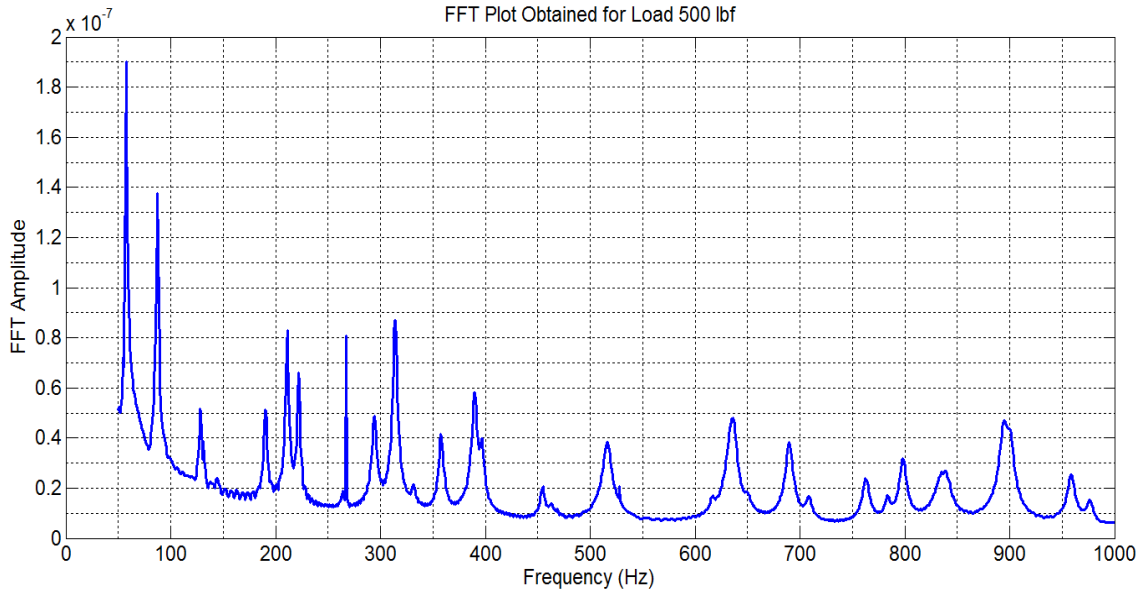


Figure 5.7. Vibration amplitude spectrum for a load of 500 lbf

Figure 5.8 and Figure 5.9 respectively show the vibration mode shapes and amplitudes corresponding to a corner load of 1000 lbf. Resonant frequencies with appreciable amplitudes are fewer in the range of 50 Hz to 300 Hz. Further, a number of minor peaks are seen in the frequency range between 300 Hz to 1000 Hz. The experimental mode shapes were quite different from the numerical results. Further, in the experimental results the $f_{1,1}$ mode seems to occur around 104 Hz, but the amplitude was very small. The $f_{1,2}$ mode occurred at around 54 Hz. The switching of the order of first and second modes was seen by other researchers (Virgin, 2006).

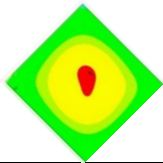
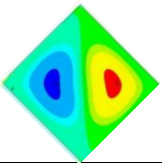
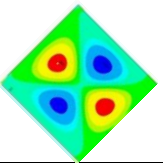
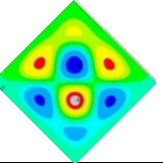
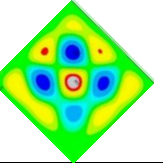
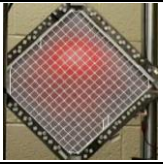
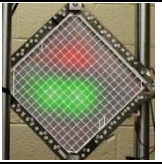
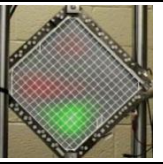
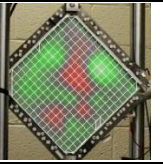
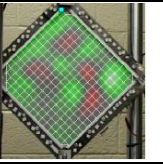
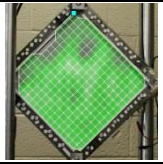
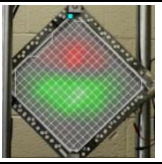
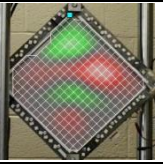
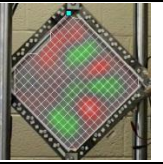
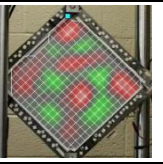
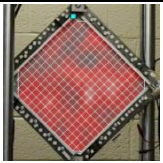
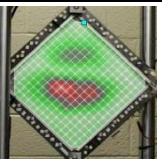
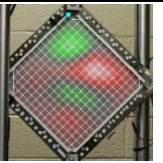
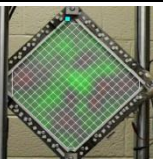
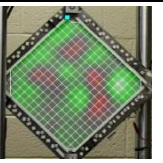
		$f_{1,1}$	$f_{1,2}$	$f_{1,3}$	$f_{1,4}$	$f_{1,5}$
FEA Mode shapes and frequencies						
		80 Hz	162 Hz	215 Hz	334 Hz	543 Hz
Experimental Mode shapes and frequencies	Trial #1					
		101 Hz	54 Hz	194 Hz	343 Hz	535 Hz
	Trial #2					
		103 Hz	54 Hz	204 Hz	343 Hz	535 Hz
	Trial #3					
		103 Hz	54 Hz	204 Hz	343 Hz	535 Hz

Figure 5.8. Mode shape and frequency comparison for a load of 1000 lbf

In comparing the amplitudes of the resonant frequencies at different load levels, in general the amplitude of oscillations were reduced as the panel underwent progressively increasing levels of buckling. At higher levels of buckling, a relatively larger number of low amplitude peaks were seen. Apparently these peaks correspond to localized oscillations of a small portion of the panel, without the whole panel participating in the resonant oscillations. This is also seen in the mode shapes. The sharp peaks seen around 270 Hz and 530 Hz in the vibration amplitude spectra were spurious readings seen in the results and do not correspond to the vibrations of the shear panel.

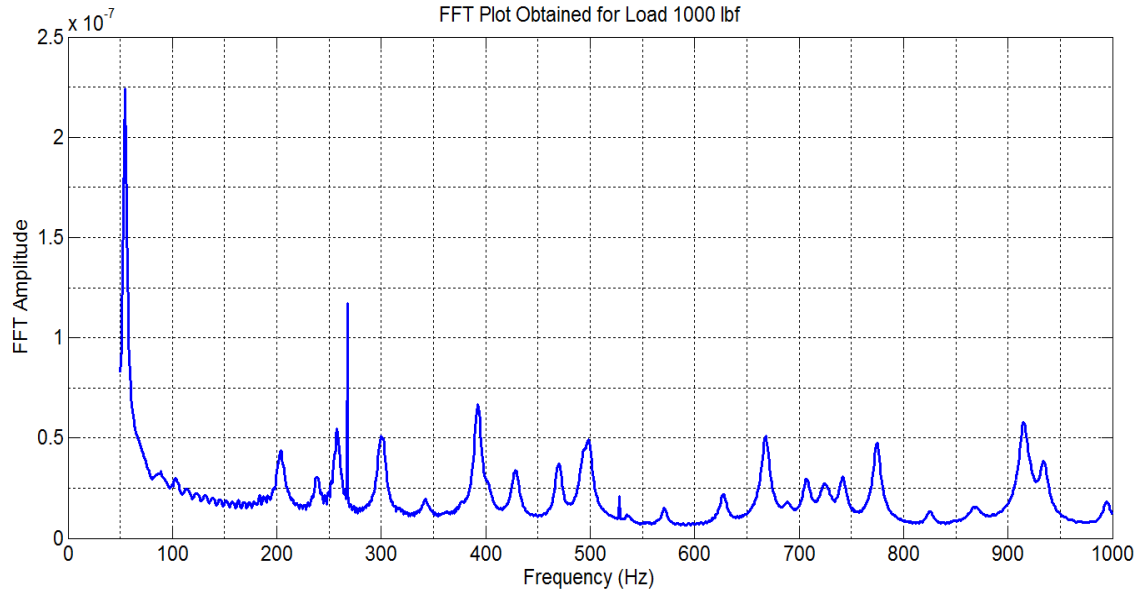


Figure 5.9. Vibration amplitude spectrum for a load of 1000 lbf

The correlation between the numerical results and experimental results was poor even for the higher order modes. The amplitude spectrum for a load of 1500 lbf is shown in Figure 5.10. The comparison of numerically generated mode shapes and experimental mode shapes for a corner load level of 2000 lbf are shown in Figure 5.11. Corresponding amplitude spectrum is shown in Figure 5.12. The interchange of the order of occurrence of $f_{1,1}$ and $f_{1,2}$ was seen at this load also in the experimental results. There is an excellent correlation for unbuckled plate resonance frequencies and the modes. There is a difference between experiment and numerical model results. The differences between the numerical and experimental mode shapes as well as frequencies would be due to the difficulty in modeling the exact boundary conditions and the nonlinear buckling behavior in the numerical modeling.

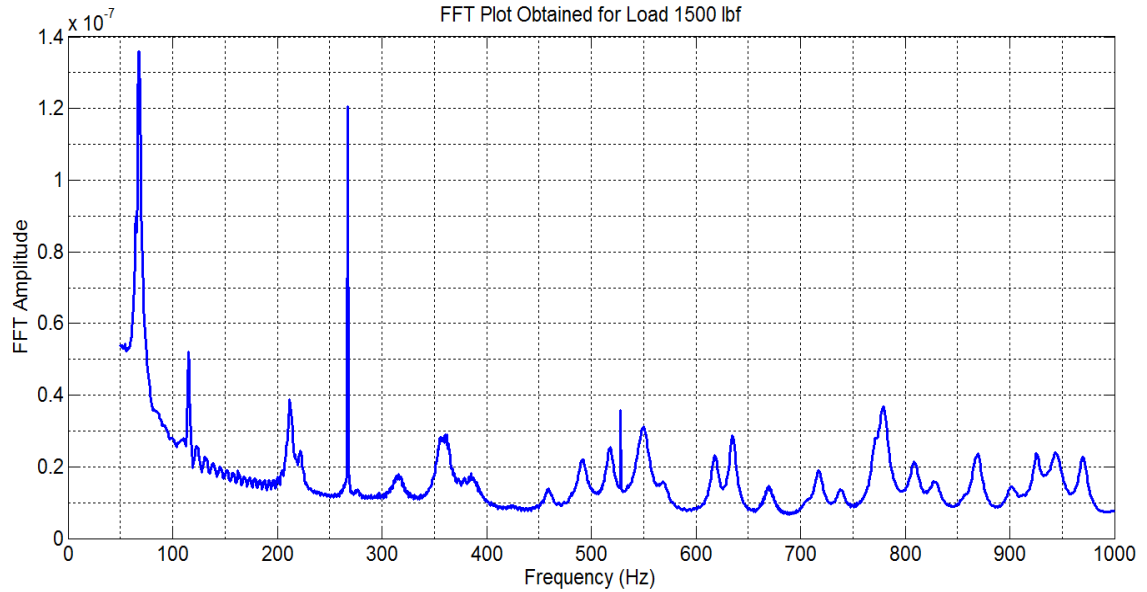


Figure 5.10. Vibration amplitude spectrum for a load of 1500 lbf

The amplitude of oscillations of the panel at different levels of buckling deformation is compared in Figure 5.13. These results were obtained with the excitation method as well as excitation voltages kept constant. Hence the amplitude spectra that are compared reflect the changes in the properties of the panel as it undergoes buckling deformation. The shifts in the natural frequencies and the changes in amplitudes of oscillations with the buckling deformation can be evaluated from these figures. These results indicate that the panel vibration amplitudes significantly decrease with the static deflection due to buckling. The number of prominent peaks, indicated with red squares, also decreases with the buckling deformation.


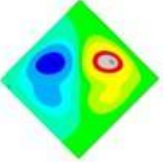
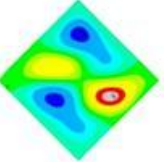
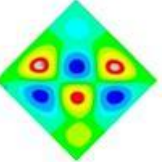
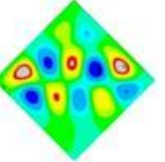



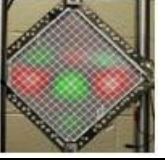
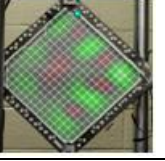
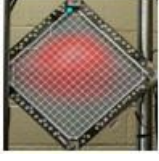
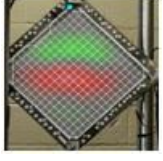
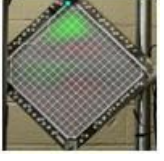

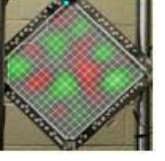


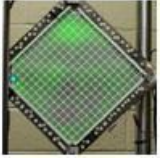
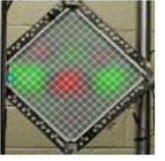
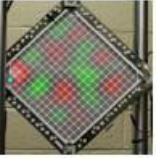
		$f_{1,1}$	$f_{1,2}$	$f_{1,3}$	$f_{1,4}$	$f_{1,5}$
FEA Mode shapes and frequencies						
		117 Hz	262 Hz	287 Hz	406 Hz	687 Hz
Experimental Mode shapes and frequencies	Trial #1					
		128 Hz	77 Hz	273 Hz	401 Hz	687 Hz
	Trial #2					
		127 Hz	78 Hz	274 Hz	404 Hz	686 Hz
	Trial #3					
		127 Hz	78 Hz	274 Hz	403 Hz	683 Hz

Figure 5.11. Mode shape and frequency comparison for the load of 2000 lbf

A comparison of the first eight resonant frequencies in their ascending order of frequencies within the frequency range of 50 Hz to 500 Hz is shown in Table 5.1. The results indicate the repeatability of the experimental results from the three trials. The gradual increase in the frequencies of those peaks with significant amplitudes can also be observed from this table.

Table 5.1. Experimental resonance frequencies (Hz) for different load levels.

	0			1000			2000		
	Trial1	Trial2	Trial3	Trial1	Trial2	Trial3	Trial1	Trial2	Trial3
1	57	59	59	54	57	54	77	78	78
2	101	104	104	101	103	103	128	127	127
3	112	115	115	194	204	204	218	222	221
4	157	162	161	244	239	239	272	273	274
5	193	199	198	254	258	257	384	384	384
6	234	240	240	307	301	300	401	403	403
7	251	256	256	343	343	342	452	456	457
8	306	313	309	402	393	392	478	478	477

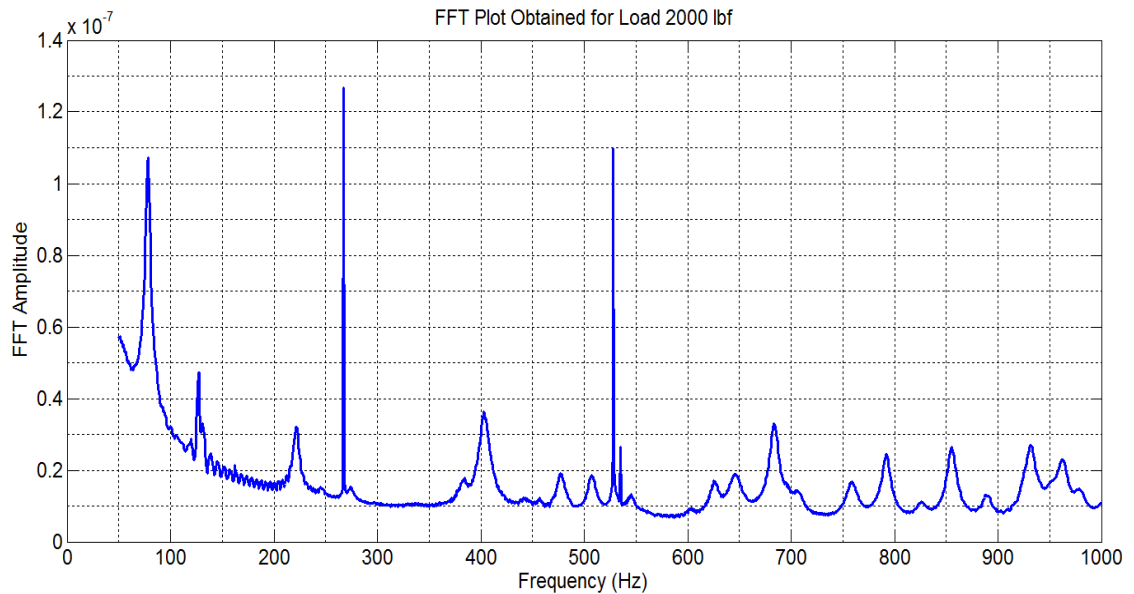


Figure 5.12. Vibration amplitude spectrum – 2000 lbf

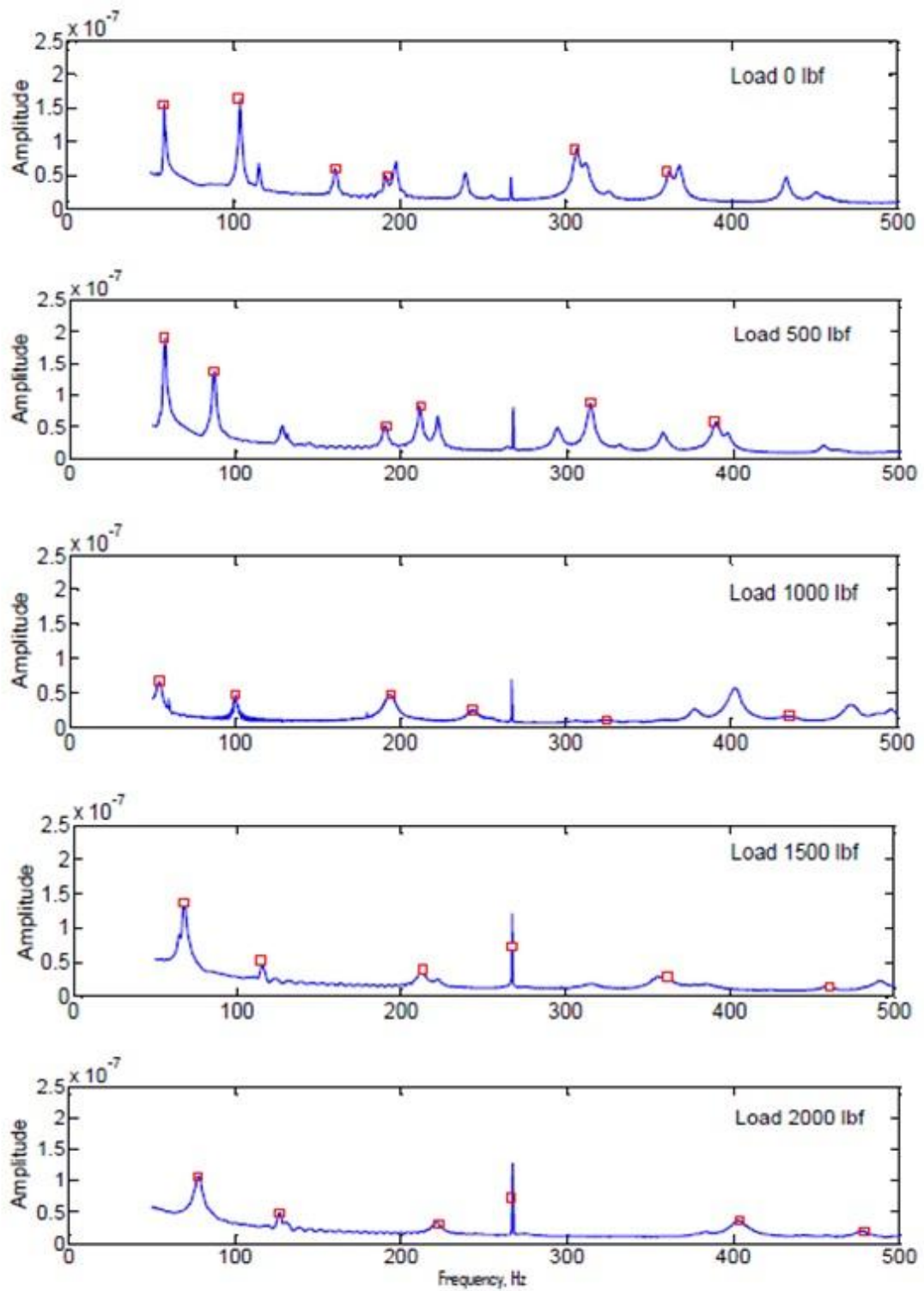


Figure 5.13. FFT Plots and Extracted Experimental Resonance Frequencies

The vibration modes seen in the experiments could not be strictly classified by the notations that are used in the description of vibrations of square panel in the form $f_{m,n}$, where the subscripts m and n respectively refer to the number of nodal lines along the two mutually perpendicular directions including the boundaries on nodal lines. Those modes which resembled closest to the modes $f_{1,1}$ to $f_{1,5}$ were selected and their frequencies are indicated as a function of buckling displacement. These modes were identified as modes 1E to 5E in this plot. This plot is shown in figure plotted in Figure 5.14. From this figure, it is clear that the first three vibration modes are the most sensitive ones for indicating the extent of buckling.

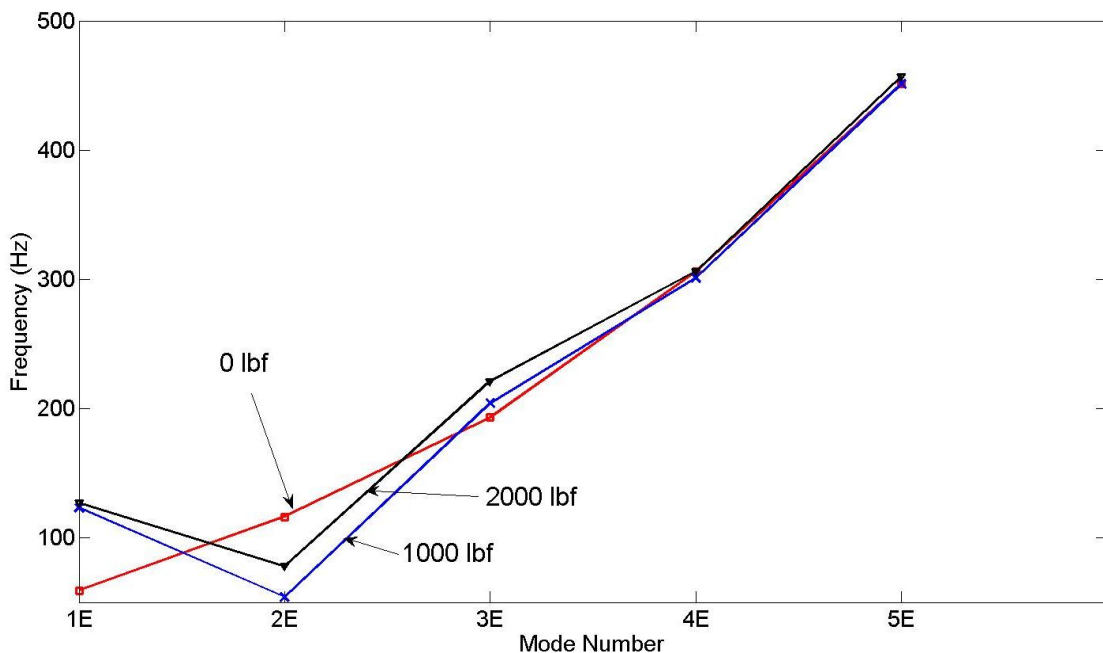


Figure 5.14. Variation of natural frequencies with load level

The frequency of the first mode has a significant increase while the frequency of the second mode first drops for the load level of 1000 lbf and subsequently increases at a load level of 2000 lbf. The frequency of the third mode shows a gradual increase with the buckling deformation. The frequencies of the 4th and the 5th modes have very low sensitivity to the buckling deformation.

5.4. Summary

The changes in the dynamic characteristics of shear panel as a result of buckling deflections is experimentally determined using a laser Vibrometer. The transverse static deflections were measured using a dial gage at a limited number of points on the plate surface. The pattern of deflections measured was in agreement with the numerical solutions. However, the magnitudes of buckling deformation obtained from the experiments were smaller than the numerical predictions.

The vibration modes as well as frequencies were measured using a laser Vibrometer. These measurements were repeated three times to verify the reproducibility. Significant changes in the natural frequencies and mode shapes were seen as the buckling initiated and progressively increased. Hence, the vibration measurement can serve as a sensitive indicator of the level of buckling. The first three modes were the most sensitive indicators of the level of buckling deformation. The drop in the frequency of the second mode with the increase in buckling deformation was a significant indicator of buckling deformation. Higher order modes could not be consistently tracked as the panel underwent increasing levels of buckling deformation in the experimental part of this study.

The results from the experiments agreed reasonably well with those from the numerical solution for the pre-buckled state. However, there was less agreement between the experimental results and numerical results in the postbuckled state. There were disagreements in the mode shapes as well as the frequencies. The drop in the frequency of the second mode seen in the experiments was not observed in the numerical results. These differences may be caused by a combination of several factors. The boundary conditions imposed in the numerical analysis may not exactly reproduce the conditions prevailing in the experiments. As the panel undergoes buckling, the edges may not be able to sustain the uniform shear stresses applied by the frame. In addition, it is known that initial imperfections affect the buckling deformation, including the shape. In the experiments, care was taken to simulate clamped boundary conditions, but there can be small deviations in the actual boundary conditions. Minor variations in the boundary conditions in the experiments and initial imperfections in the plate may have contributed to these differences.

Nonetheless, both the experimental results as well as numerical simulations indicate that vibration characteristics are sensitive indicators of the level of deformation in the postbuckling regime. Hence it may be worthwhile to explore the use of vibration based techniques to assess the margin of safety of structures operating in the postbuckled region.

CHAPTER 6

CONCLUSIONS

Structural instability is a catastrophic failure mode that is carefully considered in the design and operation of critical structures. Most structures, including those in civil infrastructure and aerospace, are prone to this failure mode. However, in many situations, beyond the initial onset of buckling, there exists a stable elastic region in which the structure can carry loads of the order of 200% of the initial buckling load. Further, the structure recovers fully elastically when unloaded from this region of loading. Reclaiming this region as a valid design space requires a full understanding of changes in the structure that take place in the postbuckled region that precedes failure. In addition, there is a critical need for a monitoring technique that can measure the extent of excursion of a given structural element into the postbuckled region and ensure that there is a sufficient margin of safety. Such a monitoring technique based on vibration characteristics of buckled structures has been proposed in this dissertation. In this research, to determine the feasibility of such an approach, the natural frequencies and mode shapes of an aluminum shear panel were monitored while the panel was undergoing different levels of buckling under uniform edge shear.

It is found that the vibration characteristics can be used as a highly sensitive indicator of the level of buckling in the case of shear panels. The changes in the resonance frequencies may be a convenient means of estimating the level of buckling. Numerical and experimental mode shapes were in agreement for the pre-buckled conditions. However, as

the buckling displacement increased, the experimental results did not correlate well with numerical results. Also, the experimental central transverse deflection plot shown in Figure 5.4 does not indicate the critical buckling load. Minor variations in the boundary conditions in the experiments and initial imperfections and the existence of diagonal tension field would be influencing parameter for these variations.

Since the experimental results found to be repeatable the results would serve as a reference for a proper development of a numerical model to include the diagonal tension effect in the numerical model. This would be possible by a numerical model of a shear plate with rigid frame.

REFERENCES

- Akesson, B., (2007), "*Plate Buckling in Bridges and other Structures*," Taylor & Francis Group.
- Ali, B., Sundaresan, M. J., Schulz, M.J., and Hughes, D., (2005), "Early Detection of Local Buckling in Wind Turbine Blades," Proceedings of SPIE Smart Structures Conference, March 6-10, San Diego
- Alinia, M. M. and M. Dastfan (2006), "Behaviour of thin steel plate shear walls regarding frame members," *Journal of Constructional Steel Research* Vol. 62, pp. 730-738.
- Alinia, M. M. and S. H. Moosavi (2009), "Stability of longitudinally stiffened web plates under interactive shear and bending forces," *Thin-Walled Structures*, Vol. 47, pp. 53-60.
- Alinia, M. M., A. Gheitasi, et al. (2009), "Plastic shear buckling of unstiffened stocky plates," *Journal of Constructional Steel Research*, Vol. 65, pp. 1631-1643.
- Alinia, M. M., and Dastfan, M., (2007), "Cyclic behavior, deformability and rigidity of stiffened steel shear panels," *Journal of Constructional Steel Research* Vol. 63, pp. 554 – 563.
- Alinia, M. M., M. Shakiba, et al. (2009), "Shear failure characteristics of steel plate girders," *Thin-Walled Structures*, Vol. 47, pp. 1498-1506.
- Alinia, M. M., S. A. A. Hosseinzadeh, et al. (2008), "Buckling and post-buckling strength of shear panels degraded by near border cracks," *Journal of Constructional Steel Research*, Vol. 64 pp. 1483-1494.
- Alinia, M.M., Habashi, H.R., and Khorram, A. (2009), "Nonlinearity in the post buckling behavior of thin steel shear panels," *Thin-Walled Structures*, Vol. 47, pp. 412 – 420.
- Annamdas, V. G. M. and C. K. Soh (2010), "Application of Electromechanical Impedance Technique for Engineering Structures: Review and Future Issues," *Journal of Intelligent Material Systems and Structures*, Vol. 21, pp. 41-59.
- ANSYS 11.0 reference manual, (2010), ANSYS Inc.
- Asamene, K., Ali, B., and Sundaresan, M., (2010), "Structural Health Monitoring Techniques for Detecting Incipient Buckling," Proc. SPIE Smart Structures/NDE Conference, March, 2010, San Diego, CA.
- Basler, K., (1960), "Welded plate girders: Strength of plate girders in Shear," Fritz Engineering Laboratory Report No. 251.20

Basler, K., Thurlimann, B., (1960), "Welded plate girders: Strength of plate girders in bending," Fritz Engineering Laboratory Report No. 251.19

Basler, K., Yen, B.T., Mueller, J.A., Thurlimann, B., (1960), "Welded plate girders: Web buckling tests on welded plate girders (part 1)," Fritz Engineering Laboratory Report No. 251.11

Basler, K., Yen, B.T., Mueller, J.A., Thurlimann, B., (1960), "Welded plate girders: Web buckling tests on welded plate girders (part 4)," Fritz Engineering Laboratory Report No. 251.14

Bazant, Z. P., Cedolin, L., (1991), "*Stability of Structures: Elastic, Inelastic, Fracture, and Damage Theories*," Oxford University Press, Inc.

Becker, J., W. Lubber, et al. (2005), "The future role of smart structure systems in modern aircraft," *Smart Structures and Systems*, Vol. 1, pp. 159-184.

Burgreen, D., (1951), "Free vibration of a pin-ended column with constant distance between pin ends," *Journal of Applied Mechanics*, Vol. 18, pp. 135–139.

Chen, H. and L. N. Virgin (2004), "Dynamic analysis of modal shifting and mode jumping in thermally buckled plates," *Journal of Sound and Vibration*, Vol. 278, pp. 233-256.

Chen, H. and L. N. Virgin (2004), "Dynamic analysis of modal shifting and mode jumping in thermally buckled plates," *Journal of Sound and Vibration*, Vol. 278, pp. 233-256.

Chen, H. and L. N. Virgin (2006), "Finite element analysis of post-buckling dynamics in plates - Part I: An asymptotic approach," *International Journal of Solids and Structures*, Vol. 43, pp. 3983-4007.

Chen, H. and L. N. Virgin (2006), "Finite element analysis of post-buckling dynamics in plates. Part II: A non-stationary analysis," *International Journal of Solids and Structures*, Vol. 43, pp. 4008-4027.

Chen, J. S., and Ro, W. C., (2010), "Deformations and Stability of an Elastica Subjected to an Off-Axis Point Constraint," *Journal of Applied Mechanics*, Vol. 77, pp. 31-36.

Ciang, C. C., J. R. Lee, et al. (2008), "Structural health monitoring for a wind turbine system: a review of damage detection methods," *Measurement Science & Technology* Vol. 19, pp. 143- 162.

Eiseley, J.G., and Luessen, G., (1963), "Flutter of thin plates under combined shear and normal edge stresses," *AIAA Journal*, Vol. 1, pp. 620-627.

- Eisley, J. G., (1964), "Large amplitude vibration of buckled beams and rectangular plates," *AIAA Journal*, Vol. 2, pp. 2207–2209.
- Emam, S. A. and A. H. Nayfeh (2004), "On the nonlinear dynamics of a buckled beam subjected to a primary-resonance excitation," *Nonlinear Dynamics*, Vol. 35, pp. 1-17.
- Emam, S. A. and A. H. Nayfeh (2009), "Postbuckling and free vibrations of composite beams," *Composite Structures*, Vol. 88, pp. 636-642.
- Falzon, B. G., and Aliabadi, M. H., (2008), "Buckling and Postbuckling of Structures: Experimental, Analytical and Numerical studies," Imperial College Press.
- Fan, W. and P. Z. Qiao (2011), "Vibration-based Damage Identification Methods: A Review and Comparative Study," *Structural Health Monitoring-an International Journal*, Vol. 10, pp. 83-111.
- Galambos, T. V., (1998), "Stability Design Criteria for Metal Structures," John Wiley and Sons.
- Hermann, T.M., Mamarthupatti, D., and Locke, J. E., (2005), "Postbuckling Analysis of a Wind Turbine Blade Substructure," *J. Solar Energy Engineering*, Vol. 127, pp. 544-552.
- Hsieh, K. H., M. W. Halling, et al. (2006), "Overview of vibrational structural health monitoring with representative case studies," *Journal of Bridge Engineering* 11, pp. 707-715.
- Huang, G. L., F. Song, et al. (2010), "Quantitative Modeling of Coupled Piezo-Elastodynamic Behavior of Piezoelectric Actuators Bonded to an Elastic Medium for Structural Health Monitoring: A Review," *Sensors* Vol. 10, pp. 3681-3702.
- Ilanko, S, (2002), "Vibration and post-buckling of in-plane loaded rectangular plates using a multi-term Galerkin's method," *Journal of Applied Mechanics*, Vol. 69, pp. 589-592.
- Keerthan, P. and Mahendran, M., (2010), "Elastic shear buckling characteristics of LiteSteel beams," *J. Construction Steel Research*, Vol. 66, pp. 1309-1319.
- Kim, J., Park, J., and Lee, T., (2011), "Sensitivity analysis of steel buildings subjected to column loss", *Engineering Structures* Vol. 33, pp. 421–432.
- Kirikera, G. R., Shinde, V., Schulz, M. J., Ghoshal, A., Sundaresan, M., and Allemang, R., (2007), "Damage localization in composite and metallic structures using a structural neural system and simulated acoustic emissions," *Mechanical Systems Signal Processing*, Vol. 21, pp. 280-297.

- Ko, W.L., and Jackson, R.H., (1991), "Combined compressive and shear buckling analysis of hypersonic aircraft structural sandwich panels," NASA Technical Memorandum 4290.
- Kundu, C. K. and J. H. Han (2009), "Vibration and Post-buckling Behavior of Laminated Composite Doubly Curved Shell Structures," *Advanced Composite Materials*, Vol. 18, pp. 21-42.
- Lee, D.-M. and I. Lee (1997), "Vibration behaviors of thermally postbuckled anisotropic plates using first-order shear deformable plate theory," *Computers and Structures*, Vol. 63, pp. 371-378.
- Leissa, A, (1969), "Vibration of Plates," NASA Special Publication-160.
- Leissa, A, (1973), "Vibration of Shells," NASA Special Publication-288.
- Lubell, A., Prion, H.G.L., Ventura, C.E., and Rezai, M., (2000), "Unstiffened Steel Plate Shear Wall Performance under Cyclic Loading," *J. Structural Engineering*, Vol. 126, pp.453-460.
- Megson, T.H.G., (2010), "Introduction to Aircraft Structural Analysis," Elsevier.
- Memarzadeh, P., Azhari, M., and Saadatpour, M.M., (2010), "A parametric study on buckling loads and tension field stress patterns of steel plate shear walls concerning buckling modes," *Steel and Composite Structures*, Vol. 10, pp. 87-108.
- Murphy, K. D., L. N. Virgin, et al. (1996), "Characterizing the dynamic response of a thermally loaded, acoustically excited plate," *Journal of Sound and Vibration*, Vol. 196, pp. 635-658.
- Murphy, K. D., L. N. Virgin, et al. (1996), "Experimental snap-through boundaries for acoustically excited, thermally buckled plates," *Experimental Mechanics*, Vol. 36, pp. 312-317.
- Murphy, K. D., L. N. Virgin, et al. (1997), "The effect of thermal pre-stress on the free vibration characteristics of clamped rectangular plates: Theory and experiment," *Journal of Vibration and Acoustics*, Vol. 119, pp. 243-249.
- Operator's Manual for Polytec Scanning Vibrometer (PSV – 200), (2008), Polytec GmbH, Waldvonn, Germany.
- Rai, D.C., (2002), "Inelastic Cyclic Buckling of Aluminum Shear Panels," *Journal of Engineering Mechanics*, Vol. 128, pp. 1233 - 1237.
- Rainieri, C. and G. Fabbrocino (2010), "Automated output-only dynamic identification of civil engineering structures," *Mechanical Systems and Signal Processing*, Vol. 24, pp. 678-695.

- Real, E., E. and Mirambell, E., and Estrada, I., (2007), "Shear response of stainless steel plate girders," *Engineering Structures* Vol. 29, pp. 1626-1640.
- Reddy, J. N., (1999), "*Theory and Analysis of Elastic Plates*," Taylor and Francis.
- Reddy, J.N., (2004), "*Mechanics of Laminated Composite Plates and Shells*," 2nd edition, CRC Press.
- Roberts, T.M., and Sabouri-Ghomi, S., (1991), "Hysteritic characteristics of unstiffened plate shear panels," *Thin Walled Structures*, Vol. 12, pp.145-162.
- Sabouri-Ghomi, S., Ventura, C.E., and Kharrazi, M. H. K., (2005), "Shear Analysis and Design of Ductile Steel Plate Walls," *J. Structural Engineering*, Vol. 131, pp. 878-889.
- Schulz, M. J., and Sundaresan, M. J., (2006), Smart sensor system for structural condition monitoring of wind turbines, *Subcontract Report*, NREL/SR-500-40089, National Renewable Energy Laboratory, CO, USA.
- Shiau, L. C. and T. Y. Wu (1997), "Free vibration of buckled laminated plates by finite element method," *Journal of Vibration and Acoustics*, Vol. 119, pp. 635-640.
- Simitses. G.J., and Hodges, D.H., (2006), "*Fundamental of Structural Stability*," Elseveir Inc.
- Singer, J., Arbocz, J., and Weller, T., (1998), "*Buckling Experiments: Experimental Methods in Buckling of Thin-Walled Structures*," Volume 1, John Wiley and Sons Ltd.
- Singer, J., Arbocz, J., and Weller, T., (2002), "*Buckling Experiments: Experimental Methods in Buckling of Thin-Walled Structures*," Volume 2, John Wiley and Sons.
- Soedel, W., (2004), "*Vibration of Plates and Shells*," Marcel-Dekker.
- Sundaresan, M. J., Schulz, M. J., and Ghoshal, A., (2002), "Structural health monitoring static test of a wind turbine blade," *Subcontract Report*, NREL/SR-500-28719, National Renewable Energy Laboratory, CO, USA.
- Sundaresan, M.J., Schulz, M.J., and Ghoshal, A., March 2002, "Structural Health Monitoring Static Test of a Wind Turbine Blade," National Renewable Energy Laboratory Technical Report, NREL/SR-500-28719.
- Taha, M. M. R., A. Nouredin, et al. (2006), "Wavelet transform for structural health monitoring: A compendium of uses and features," *Structural Health Monitoring-an International Journal*, Vol. 5, pp. 267-295.
- Thompson, J.M.T., and hunt G.W., (1984), "*Elastic Instability Phenomena*," John Wiley and Sons.

Tilmans, H. A. C., M. Elwenspoek, et al. (1992), "Micro resonant force gauges," *Sensors and Actuators A: Physical*, Vol. 30, pp. 35-53.

Timoshenko, S., Gere, J., (1985), "*Theory of Elastic Stability*," McGraw-Hill International Book Company, 17th Edition.

Virgin, L.N., 2007, "*Vibration of axially loaded structures*," Cambridge University Press, NY.